History shapes regulatory and evolutionary responses to tigecycline in strains of *Acinetobacter baumannii* from the pre- and post-antibiotic eras

Alecia B Rokes[1,2], Alfonso Santos-Lopez[3], Vaughn S Cooper[1,2]

[1]University of Pittsburgh, Department of Microbiology and Molecular Genetics, Pittsburgh, PA, USA

[2]Center for Evolutionary Biology and Medicine, University of Pittsburgh, Pittsburgh, PA, USA

[3]Department of Molecular Biology, Autonomous University of Madrid, Madrid, Spain

ASL
ORCID: 0000-0002-9163-9947
ABR
ORCID: 0000-0001-9496-0296
VSC
ORCID: 0000-0001-7726-0765

History shapes regulatory and evolutionary responses to tigecycline in strains of *Acinetobacter baumannii* from the pre- and post-antibiotic eras

ABSTRACT

Evolutionary history encompasses genetic and phenotypic bacterial differences, but the extent to which history influences drug response and antimicrobial resistance (AMR) adaptation is unclear. Historical contingencies arise when elements from an organism's past leave lasting effects on the genome, altering the paths available for adaptation. We utilize strains isolated before and after widespread antibiotic use to study the impact of deep historical differences shaped by decades of evolution in varying antibiotic and host pressures. We evaluated these effects by comparing immediate and adaptive responses of two strains of *Acinetobacter baumannii* to the last-resort antibiotic, tigecycline (TGC). When grown in subinhibitory TGC, the two strains demonstrated divergent transcriptional responses suggesting that baseline transcript levels may dictate global responses to drug and their subsequent evolutionary trajectories. Experimental evolution in TGC revealed clear differences in population-genetic dynamics – with hard sweeps in populations founded by one strain and no mutations reaching fixation in the other strain. Transcriptomes of evolved populations no longer showed signatures of drug response, as was seen in the ancestors, suggesting that genetic adaptation may outweigh preexisting differences in transcriptional networks. Genetically, AMR was acquired through predictable mechanisms of increased efflux and drug target modification; however, the two strains adapted by mutations in different efflux regulators. Fitness tradeoffs of AMR were only observed in lineages evolved from the pre-antibiotic era strain, suggesting that decades of adaptation to antibiotics resulted in preexisting compensatory mechanisms in the more contemporary isolate, an important example of a beneficial effect of historical contingencies.

SIGNIFICANCE STATEMENT

Acinetobacter baumannii is a high priority pathogen often causing multidrug resistant nosocomial infections. Many healthcare systems experience clonal outbreaks of *A. baumannii* infections, yet treatment strategies are often strain-agnostic, ignoring the importance of strain differences. We show that historical differences between two strains, one isolated prior to widespread antibiotic use and the other following decades of selection to clinical conditions, dictate transcriptional patterns and response to a last-resort antibiotic and influence the genetic and phenotypic routes of resistance adaptation. While our study focuses on two reference strains of *A. baumannii,* these findings can be more broadly applicable to other pathogenic organisms in which a better understanding of the forces influencing resistance adaptation is essential for combating the antimicrobial resistance crisis.

39

40 **INTRODUCTION**

41 Evolution is an inescapable process, as the worsening antimicrobial resistance (AMR)
42 crisis demonstrates (1). However, the AMR crisis will be less daunting if we are better able to
43 understand, predict, and direct the evolutionary outcomes of antibiotic treatment (2, 3). With
44 better resolution of factors affecting the routes to resistance, we may be able to work toward
45 directing evolution to avenues with exploitable resistance tradeoffs (4, 5). However, genotypic
46 and phenotypic routes to resistance, as well as the resulting fitness tradeoffs, may be highly
47 influenced by strain history, decreasing the range and applicability of evolutionary strategies to
48 counteract the evolution of AMR (6, 7).

49 There are three primary forces, often intertwined, that influence evolution: history,
50 chance, and selection (5, 8, 9). Natural selection causes the most fit alleles in a population to
51 rise in frequency while less fit mutants are lost from the population. Selection needs heritable
52 phenotypic variance to act upon that is produced by mutations arising randomly, a factor of
53 chance. Chance events also occur in the demography of microbial populations, such as
54 population bottlenecks arising during infections (10). The outcome of a mutation is also
55 affected by the genetic background in which it arises (11, 12), combining chance and the final
56 force of evolutionary history, which can influence adaptation in diverse ways but remains
57 understudied.

58 Evolutionary history encompasses the genetic and phenotypic remnants from a
59 bacterium's past including biotic and abiotic factors, such as interactions with other cells and
60 previous environmental exposures like antibiotics, respectively (13). The phylogenetic origin of
61 the bacterium is also a major component of evolutionary history. These differences can impose
62 historical contingencies through which preexisting elements in the genome, transcriptome, or
63 phenome alter or constrain evolutionary paths available for adaptation (13, 14). History may
64 dictate the type, identity, rate, and order of mutations acquired (15–18). Additionally, history
65 likely influences fitness and phenotype associated with a mutation, thereby dictating
66 evolutionary trajectories and outcomes (19–21). This study seeks to understand how historical
67 contingencies influence evolutionary trajectories under the strong selective pressure of
68 antibiotic treatment (22).

69 Contingencies imposed by history exacerbate our inability to accurately predict bacterial
70 responses to antibiotics and AMR evolution. *Acinetobacter baumannii* is a nosocomial pathogen
71 of increasing concern due to limited and often ineffective treatment options (23). With time
72 and increased antibiotic use, strains of *A. baumannii* have acquired mutations and mobile
73 genetic elements, on top of many conserved genes, that endow desiccation resistance, stress
74 tolerance, and drug resistance (24, 25). Such historical differences could cause archaic strains,
75 which are often represented by laboratory reference strains, to respond and evolve differently
76 than contemporary infectious strains (26, 27). Importantly, hospitals typically experience clonal

77 outbreaks of *A. baumannii* caused by closely related isolates of the same sequence type (28,
78 29). Across hospital systems, *A. baumannii* infections exhibit high diversity (30, 31), but only a
79 handful of treatments are used. This practice ignores the importance of genetic background
80 and evolutionary history in the treatment process, likely leading to differences in treatment
81 response (32, 33). A better understanding of how various strains respond and adapt to
82 antibiotics would result in improved patient outcomes.
83 The widespread use of antibiotics in clinical practice has dramatically affected pathogen
84 evolution (7, 34). Comparing strains isolated before and after the clinical introduction of
85 antibiotics provides an excellent framework to study how deep historical differences influences
86 the evolution of resistance (35). To this end, we used two strains of *A. baumannii,* one that was
87 isolated early in the antibiotic era and has not been exposed to many contemporary antibiotics,
88 and one that is better representative of current multi-drug-resistant (MDR) clinical infections
89 having been isolated much more recently. Comparing these strains enables assessment of how
90 a history of evolving with the human host and novel antimicrobial pressures impacts resistance
91 evolvability.
92 Resistance adaptation can be investigated at multiple levels: from the narrowest, the
93 site-specificity of individual mutations, to more systematic resistance pathways, and even more
94 broadly, at the level of population-wide responses and adaptive dynamics (36, 37). This study
95 looks within and across these levels to determine the areas in which evolutionary history is
96 most influential. We find that deep history influences the basal transcriptome, driving
97 differences in the response to TGC. The strains also differed in their evolved responses to
98 prolonged TGC stress at both narrow molecular-genetic and broader population-genetic levels,
99 despite superficial similarities. This work highlights the importance of evolutionary history in
100 the response and adaptation of a high-priority pathogen to a last-resort antibiotic, showing that
101 strain differences can reduce the predictability of treatment outcomes.
102
103 **RESULTS**
104 Genomic and phenotypic classifications of the strains
105 Previous studies of historical differences in strain response to antibiotics have used
106 strains separated by relatively few mutations (9). Here, we study effects of deeper history on
107 the evolution of AMR in two different *A. baumannii* strains isolated nearly 60 years apart, *i.e.*
108 before and after the widespread clinical use of antibiotics. The first strain, 17978UN, is a variant
109 of the commonly used laboratory reference strain ATCC 17978 (38). This strain was isolated in
110 1951 in the early stages of the introduction of antibiotics in clinical practice (39). In contrast,
111 the second strain, AB5075-UW, is a variant of AB5075, which was isolated in 2008 from a MDR
112 infection representative of the current global clinical burden of *A. baumannii* (40, 41).
113 Therefore, the evolutionary histories of both strains have likely been shaped by different
114 exposures to antibiotics, hospitals, and the human host. In many ways 17978UN represents

115 archaic *A. baumannii* infections in comparison to contemporary MDR infections represented by
116 AB5075-UW.
117 We first characterized genomic and phenotypic differences between the two strains to
118 evaluate their historical distinctions. 17978UN is a member of sequence type ST437 whereas
119 AB5075-UW is assigned to ST1, part of the clinically dominant clonal complex 1 (40). Their
120 genomes share an average nucleotide identity of 97.5% and 3265 homologous core genes.
121 17978UN contains an additional 694 accessory genes whereas AB5075-UW encodes 751
122 accessory genes (Data S1), with no significant differences in gene content grouped by Clusters
123 of Orthologous Genes (COG) categories (Table S1). However, as expected by its lineage and
124 history of antibiotic exposure, AB5075-UW has significantly more resistance-associated
125 elements than 17978UN (Table S1) and is more resistant to a variety of antibiotics (Table S2).
126 Notably, both strains were susceptible to at least two different classes of antibiotics.
127 These significant differences in genome content and existing AMR led to the hypothesis
128 that the strains would respond differently to a contemporary, clinically relevant antibiotic.
129 Tigecycline (TGC) is a translation-inhibiting antimicrobial compound that was approved for
130 clinical use in 2005 (42). Resistance to TGC in clinical isolates of *A. baumannii* is typically
131 attributed to overexpression of efflux pumps or ribosomal modifications (43, 44). The minimum
132 inhibitory concentration (MIC) of TGC differed only slightly between the strains (17978UN
133 MIC_{TGC} = 0.125 µg/mL, AB5075-UW MIC_{TGC} = 0.25 µg/mL). Further, subinhibitory TGC (0.06
134 µg/mL) imposed approximately 75% and 60% fitness defects in 17978UN and AB5075-UW,
135 respectively (Fig. S1). This comparable level of growth inhibition by TGC enables the study of
136 influences of deep evolutionary history on both transcriptional response and subsequent
137 evolutionary adaptation.
138
139 <u>Strain-dependent transcriptional response acts on historically differentially utilized genes</u>
140 Given the stress imposed on growth by TGC, even at subinhibitory levels, we predicted
141 that transcriptional responses to this drug would be largely conserved between strains, likely
142 consisting of stress-response genes, drug resistance mechanisms, or ribosomal genes specific to
143 the mechanism of action of TGC (45, 46). We compared transcript levels following growth in
144 subinhibitory TGC to growth in minimal media lacking antibiotic. The defined minimal media
145 used here and throughout was M9 salts buffered supplemented with glucose, amino acids, and
146 other elements as described in the methods (47). As expected, TGC stress caused large
147 transcriptional changes biased toward gene downregulation in both strains, but there was
148 surprisingly minimal overlap among differentially expressed genes between strains (Fig. 1 *A* and
149 *B*). Only 144 genes, representing 24% of the total downregulated genes, and 53 genes,
150 representing 18% of upregulated genes, were differentially expressed in the same direction in
151 both strains. One might intuit that the limited shared response to drug may have resulted from
152 transcriptional differences among strain-specific genes, but this was not the case. Rather, most

153 genes that were differentially expressed were within the shared genome (Fig. 1 *A* and *B*; Data
154 S1), including many genes with the greatest changes in expression that shifted in opposite
155 directions between strains (Fig. S2 and Fig. S3). Together these results show that the response
156 to TGC stress is historically contingent.
157 To test whether baseline transcriptional differences explained varied strain response to
158 TGC, we compared transcript abundance of conserved genes in the absence of drug (Fig. 1*C*,
159 *left*). This comparison revealed differences in baseline transcriptional state that, upon TGC
160 pressure, caused expression to converge upon a common pattern of gene usage (Fig. 1*C*, *right*).
161 Genes with higher basal transcription in each strain were preferentially downregulated within
162 that strain in response to TGC treatment (Fig. 1*C*; Fig. S4), producing a more conserved
163 transcriptional state under TGC pressure (Animation S1). These historical differences in basal
164 gene expression explain the strain-dependent responses to TGC pressure.
165
166 <u>Experimental evolution for tigecycline resistance results in strain-dependent tradeoffs between</u>
167 <u>fitness and resistance</u>
168 Given the genomic signatures of history seen in the transcriptional response to TGC, we
169 hypothesized that evolutionary adaptation to this antibiotic would proceed along different
170 paths in each strain. We propagated three replicate populations of both strains for 12 days in
171 increasing concentrations of TGC (methods and Fig. S5). All populations evolved excess
172 resistance beyond the drug concentration in the media, which was maintained throughout the
173 experiment, such that all populations became nearly five times more resistant to TGC than their
174 respective ancestors (Fig. 2).
175 Antibiotic resistance is often associated with a fitness cost and these costs can depend
176 on the strain background (17, 48–50). We expected to find fitness deficits of TGC-evolved
177 populations when grown in the absence of drug, whereas we expected higher fitness of TGC-
178 evolved populations than their respective ancestors when grown in subinhibitory TGC. As
179 expected, both sets of evolved populations exhibited substantial fitness increases in
180 subinhibitory TGC. However, evolved fitness responses in the absence of drug differed.
181 Populations derived from the laboratory reference strain, 17978UN, incurred a 25-50%
182 reduction in fitness, whereas no measurable fitness cost was observed for populations derived
183 from the more recently isolated clinical strain, AB5075-UW (Fig. 2). These results show that
184 evolutionary tradeoffs between fitness and resistance to TGC differ by founding strain; and
185 suggest that contemporary MDR strains may adapt to new drugs with limited collateral fitness
186 costs.
187
188 <u>Varying population dynamics within conserved mechanisms of TGC resistance</u>
189 The divergent relationships between fitness and resistance indicated that the genetic
190 pathways to TGC resistance may differ between the two strains. We used longitudinal whole-

population, whole-genome sequencing to investigate the population-genetic dynamics of adaptation. Following prior evolution experiments in antibiotics (47, 51), we predicted that antibiotic pressure in well-mixed populations would be sufficiently strong that mutations providing resistance should rapidly sweep within the population. Indeed, mutations in genes associated with drug resistance rapidly fixed in all populations of AB5075-UW (Fig. 3; Data S2), but surprisingly, no mutations reached fixation in populations of 17978UN. A closer inspection of the mutations in each 17978UN line suggests that in total, they represent a soft sweep of resistance-associated mutations. Soft sweeps occur when multiple independent sub-lineages acquire mutations in the same genes; individual mutations never reach fixation, but the sum of all co-existing analogous mutations in a gene or pathway approach fixation within the population (52).

The evolved mutations pointed to two primary mechanisms of resistance to TGC: modification of the enzymatic target of the drug, the ribosome, and decreasing the intracellular concentration of antibiotic, primarily through efflux pumps. All replicate populations of both strains featured high-frequency mutations affecting the same pathways for drug resistance and even in the same gene. This gene encodes a *S*-Adenosyl-methionine-dependent methyltransferase (SAM-MT; Fig. 3*A*) that has been associated with creating methylation patterns required for TGC binding to the ribosome (53). Interestingly, all SAM-MT mutations that reached high frequency under TGC stress were gene disruptions caused by mobilized insertion sequences that are predicted to eliminate function (Data S2). Although each population acquired mutations in the same SAM-MT, the specific insertion sequence causing the loss of function as well as the site of insertion varied among lineages, with more variability within populations of AB5075-UW. In addition to the SAM-MT, other genes related to the target of TGC acquired mutations, such as ribosome recycling factors (Fig. 3*A*; Data S2) that likely aid in rescuing stalled ribosomes (43).

All populations also evolved mutations in regulators of efflux pumps, but the specific resistance-nodulation-division (RND) pump that was affected differed between strains. Populations of 17978UN also acquired mutations affecting other systems predicted to reduce intracellular concentrations of TGC. For instance, two 17978UN populations acquired mutations in major facilitator superfamily (MFS) transporters that rise to high frequency (Fig. 3*B;* Data S2) (54). In summary, the identities, timing, and frequencies of evolved mutations differed between strains, whereas replicate populations founded by the same strain exhibited high gene-level parallelism.

<u>Strain-dependent efflux pump preferences</u>

All populations adapted to TGC through mutations in drug efflux systems (Fig. 3*B*), yet different strains evolved with different genetic signatures. *A. baumannii* encodes three RND-efflux pumps known to be associated with drug resistance adaptation (55, 56). Two-component

229 system *adeRS* regulates efflux operon *adeABC,* while the other two pumps, *adeFGH* and *adeIJK*
230 are regulated by negative regulators *adeL* and *adeN,* respectively (Fig. 4*A*) (57). Both strains
231 encode all three pumps with a high level (97-100%) of amino acid conservation (Table S2), with
232 the only exception that 17978UN does not encode the outer membrane protein, AdeC, but
233 AdeK can complement function (55). Populations of AB5075-UW acquired nonsynonymous
234 mutations throughout the *adeRSABC* efflux system, altering *adeA*, *adeB*, and *adeS*. One of two
235 predominant single nucleotide polymorphisms (SNPs) in *adeS* (R152K and G160S) fixed in all
236 AB5075-UW populations, and an additional SNP in *adeB* (E939Q) was nearly fixed in one
237 population (Data S2). In contrast, each evolved 17978UN population acquired mutations in
238 *adeL* caused by an insertion sequence (IS) disruption in this gene that rose to high frequency
239 (Fig. 3*B*; Data S2). This disruption exhibited site-specific parallelism in which the mutation was
240 identical within all three TGC-evolved populations, but never reached 100% frequency. As an
241 example of the soft sweep dynamics described previously, in evolved population 3 we observe
242 an additional mutation in *adeL* and the two mutations in this gene, cumulatively, reach fixation.
243 Interestingly, a nonsynonymous SNP in *adeR* also arose in 17978UN populations 1 and 3 on day
244 three but it was quickly outcompeted by *adeL* mutations (Fig. 3*B*), further emphasizing the
245 strain-dependence of efflux mutations.
246 There are many ways in which historical contingencies could cause such strain-specific
247 preferences of efflux targets. One possibility is that the sequences of these target genes had
248 already differentiated, but all sites that acquired adaptive mutations were initially identical in
249 the ancestral genomes (Table S3). Another possibility is that the ancestral strains had previously
250 evolved differential regulation of these pumps by other mechanisms. To test this notion, we
251 measured expression of efflux genes in the presence and absence of subinhibitory TGC but
252 found comparable levels of expression of *adeABC* and *adeFGH* (Fig. 4*B*), discounting this
253 explanation. We found that 17978UN exhibits relatively greater expression of the *adeIJK* pump
254 in both growth conditions, but this pump was not the target of selection in either strain. In the
255 absence of TGC, 17978UN had increased efflux activity compared to AB5075-UW (Fig. 4*C*),
256 possibly due to the differences in AdeIJK expression. Interestingly, drug pressure induced
257 significantly different states of efflux activity, increasing efflux activity in AB5075-UW but
258 decreasing it in 17978UN (Fig. 4*C*). As expected, there were significant differences in efflux
259 activity and expression in the evolved populations, confirming that the mutations in efflux
260 regulators produced a meaningful phenotype. All evolved populations, except 17978UN
261 evolved population 3 which still trended higher, evolved significantly increased efflux activity
262 than their respective ancestors (Fig. 4*D*). Lastly, we show that the mutated regulators
263 specifically increase expression of their associated pump (Fig. 4*E*). In summary, neither
264 sequence divergence nor functional differences in the primary targets of selection explained
265 the alternative evolutionary pathways to increased drug efflux. These results strongly suggest

266 that more complex interactions between efflux systems and the genome favor different routes
267 to drug adaptation.
268
269 Diminished transcriptional response and historical influences following TGC adaptation
270 The ancestral strains exhibited divergent transcriptomic changes in response to TGC
271 stress (Fig. 1), but both adapted to TGC via broadly similar mechanisms. To evaluate the
272 transcriptional signature of evolved drug tolerance, we conducted RNA sequencing of evolved
273 populations grown with or without TGC treatment and found remarkably few differences (Fig.
274 5*A*). Compared to the ancestral response, where many genes changed in abundance upon TGC
275 treatment, all evolved populations exhibited nearly identical transcriptomes in the two
276 conditions. This trend is more conspicuous in populations of AB5075-UW, where no genes are
277 significantly different (p-value < 0.05 and absolute value log fold change > 1) between the two
278 conditions, while a few genes remain significantly differently expressed upon TGC stress in
279 populations of 17978UN (Fig. S6, Data S3).
280 While the muted transcriptional response to drug is observed in all evolved populations,
281 it does not tell us if evolved transcriptional responses are conserved between strains. Principal
282 component analysis of transcript abundance confirmed that TGC treatment shifts the initially
283 diverging ancestral transcriptomes in the same direction while still preserving strain differences
284 (Fig. 5*B*). Transcriptomes of evolved populations, either treated or untreated, strongly grouped
285 together. This cluster of evolved populations groups more closely with the untreated ancestors,
286 further supporting limited transcriptional response to TGC stress by evolved populations (Fig.
287 5*B*; Fig. S6). Taken together, these convergent evolved transcriptomes show that genomic drug
288 adaptations alleviate the need to transcriptionally respond to TGC pressure and result in
289 reduced historical signatures on the transcriptome compared to the divergent ancestral
290 transcriptomes.
291
292 **DISCUSSION**
293 Antimicrobial resistance (AMR) is a problem of evolution that is most often observed in
294 retrospect, when treatment fails. We still have much to learn about how AMR evolves,
295 including the diversity of genetic pathways to resistance (22), the extent to which these
296 pathways depend on the environment (47) including the host immune status (58), and whether
297 these pathways differ among historically divergent strains (18, 20). In this study, we focused on
298 this last factor by evaluating how reference strains isolated nearly 60 years apart, spanning eras
299 of antibiotic usage, differ in their adaptation to a clinically significant drug. Although both
300 strains of *A. baumannii* adapted to grow in media containing tigecycline (TGC) via common
301 pathways, the specific genes and mutations differed with the founding strain. On the other
302 hand, replicate populations derived from the same strain evolved in parallel, indicating a level
303 of genetic predictability within but not between strains.

304 Perhaps the most striking difference between strains was the fitness consequence of
305 TGC adaptation: lineages derived from the modern clinical strain experienced no measurable
306 fitness costs whereas those derived from the historical strain, 17978UN, incurred deficits of
307 25% or more (Fig. 2). Fitness effects are often related to the stability or persistence of
308 resistance. Costly resistance has long been proposed as a beneficial trait for humanity that can
309 preserve drug efficacy in the face of selection (3, 59, 60). Here we find an alarming lack of a
310 fitness cost of evolved resistance in lineages derived from the contemporary clinical isolate,
311 AB5075-UW. The evolutionary history of AB5075-UW includes frequent antibiotic exposure
312 prior to our studies that could have selected for compensatory adaptations that alleviate costs
313 of TGC resistance (61). The lack of a fitness-resistance tradeoff in AB5075-UW suggests that
314 passive loss of resistance once drug pressure is alleviated will be rare in related strains,
315 increasing the need for alternative treatment options.
316 Differences in the genetic causes of resistance between strains offer evidence that
317 historical contingency influences routes to AMR. Many bacterial genomes including *A.*
318 *baumannii* encode multiple RND efflux pumps and to explain this apparent redundancy, a
319 hierarchical model of sequential activation has been proposed (54, 57, 62). We find that the
320 first, dominant mutations affecting drug efflux in each strain affected regulators of different
321 pumps, with SNPs in *adeS* sweeping to fixation in AB5075-UW populations and gene disruptions
322 caused by IS in *adeL* reaching high frequencies in 17978UN populations (Fig. 3). This suggests
323 that the hierarchy of these pumps differs between strains in the face of TGC pressure and raises
324 the possibility that variation in their regulatory network or gene content evolved in the past.
325 Perhaps the diminished priority of the AdeRSABC pump in 17978UN stems to the lack of *adeC* in
326 this strain (Fig. 4*A*; Data S1). These lineages would need to accumulate two mutations to
327 overexpress one functional pump: one that upregulates AdeAB and one that upregulates AdeK
328 to serve as the outer membrane protein (55). The historical contingency imposed from the loss
329 of *adeC* sometime in the history of 17978UN may be driving the strain-dependent efflux
330 preferences for drug adaptation.
331 Both the spectra of evolved mutations and their dynamics differed between strains,
332 suggesting intrinsic biases that influence genetic diversity. Despite having the same number of
333 encoded insertion sequences (IS) as AB5075-UW (Table S1), nearly all high-frequency mutations
334 in populations of 17978UN were caused by IS interrupting open reading frames, whereas
335 populations of AB5075-UW experienced a greater diversity of mutation types. IS elements are
336 known to play an important role in *A. baumannii* mutagenesis (63). The strain-dependent
337 historical contingencies on insertion sequence mobilization, repertoire, and insertion site could
338 have lasting impacts on the future stability of these mutations and, therefore, the stability of
339 resistance stemming from IS mediated mechanisms (63, 64). Further, resistance-associated
340 mutations fixed in populations of AB5075-UW, but no mutations fixed in populations of
341 17978UN, indicating coexisting lineages. The maintained diversity in 17978UN lineages may be

342 due to relatively greater mutation availability causing the coincident rise of multiple adapted
343 lineages. When multiple mutations in the same gene collectively reach fixation, this
344 phenomenon is known as a soft sweep (65, 66). At the population level, the diversity
345 maintained in a population undergoing selection from antibiotics is an important indicator of
346 future paths available for additional adaptation in new environments. In this regard,
347 populations of 17978UN may be more evolvable when challenged with a new stress.
348 It would be ideal to be able to predict evolutionary trajectories of AMR from patterns of
349 transient response to an antibiotic. While we do not see clear signatures that may enable
350 predictions of drug adaptation at the gene level (45), our work shows that strain background
351 greatly influences transcriptomic response to antibiotics. The large transcriptomic differences
352 between strains in the absence of drug, which in turn influenced their responses to TGC (Fig. 1),
353 was remarkable and could be used to map functional contingencies between strains. Many
354 more transcriptomes of additional strains would be needed to evaluate the power of
355 transcriptomes as markers of evolutionary history and to anticipate drug responses.
356 Nonetheless, our studies suggest the existence of a conserved transcriptional state under TGC
357 stress that different unexposed cell-states migrate toward. The conserved transcriptomes of
358 evolved populations harboring several new AMR mutations further support a homogeneous
359 state associated with drug adaptation (Fig. 5). We noted that the evolved transcriptomes more
360 closely represent the untreated ancestral state, suggesting that the evolved populations are,
361 essentially, not feeling the pressure of the antibiotic, likely due to the adaptations in drug efflux
362 decreasing the intracellular concentrations of TGC (Fig. 4). It would be valuable to test if the
363 collapse of transcriptional heterogeneity upon transient antibiotic pressure as well as
364 prolonged adaptation is a general pattern or is contingent on the class or concentration of
365 antibiotic applied. A lack of transcriptional response to antibiotics in clinically adapted samples
366 could be used as another biomarker upon which to predict the extent of genetic resistance
367 adaptation.
368 In a world shifting toward personalized medicine, we should also shift treatment of
369 infections to be tailored to the specific strain or sequence type causing the infection. This work
370 supports the idea that initial responses as well as evolutionary trajectories to antibiotic stress
371 can be highly strain-dependent, and therefore, treatments should be as well. If we are better
372 able to predict the impact of historical contingencies in the transcriptional response and in
373 fitness tradeoffs associated with AMR evolution, we will be one step closer to personalized
374 treatment of MDR infections.
375
376 **METHODS**
377 Bacterial strains and growth conditions
378 Laboratory reference strain ATCC 17978UN (38, 39) and clinical reference strain
379 AB5075-UW (40, 41) were used throughout the study and grown under the same conditions.

380 Unless otherwise stated, bacterial cultures were grown in 5ml M9+ media, as previously
381 described (47). Briefly, M9+ media is a salts-buffered media with glucose (11.1mM) as the
382 primary carbon source. It contains 0.1 mM $CaCl_2$, 1 mM $MgSO_4$, 42.2 mM Na_2HPO_4, 22 mM
383 $KH2PO_4$, 21.7 mM NaCl, 18.7 mM NH_4Cl and is supplemented with 20 mL/L MEM essential
384 amino acids (Gibco 11130051), 10 mL/L MEM nonessential amino acids (Gibco 11140050), and
385 1 mL each of trace mineral solutions A, B, and C (Corning 25021–3 Cl). Cultures were incubated
386 at 37°C with shaking or on a roller-drum at approximately 250rpm.
387
388 Genomic comparison of the two strains
389 Genomes were annotated with bakta (v1.6.1, database v4.0) (67) and input to Panaroo
390 (v1.3) in the sensitive clean mode to obtain a gene presence/absence list that included plasmid
391 encoded genes (68). We assessed pairwise nucleotide similarity of the two strains with pyANI
392 (v0.2.12; (69). Multilocus sequence types were confirmed using mlst (v2.11;
393 https://github.com/tseemann/mlst) (70). Elements associated with resistance, including known
394 single nucleotide polymorphisms (SNPs), were detected with AMRfinderPlus (version 3.11.26
395 with database version 2023-11-15) (71). Two-proportion z-tests on two-tailed hypotheses were
396 used to determine if gene content was significantly different in the two strains, accounting for
397 the difference in genome size (Table S1). The annotated reference genomes used in this study
398 can be found in the NCBI BioProject ID PRJNA1214285.
399
400 Measuring resistance
401 Broad resistance profiles of the two strains were determined using Sensitire plates
402 (ThermoFisher, GN3F) following the manufactures protocols. Minimum inhibitory concentration
403 (MIC) assays were performed to measure susceptibility levels more accurately to Tigecycline
404 (TGC, Sigma 220620-09-7) following modified CLSI methods (9, 72). More detailed methods can
405 be found in the supplement.
406
407 RNA extraction and purification
408 Cultures for transcriptomic analysis of the ancestor strains were seeded from individual
409 colonies in biological triplicate into 5mL M9plus media. Population cultures were started
410 directly from the freezer stock into 5mL M9plus to avoid unnecessary outgrowths. Dilutions of
411 the cultures into M9plus with or without TGC treatment at 0.06 µg/mL were grown to mid-late
412 exponential phase for RNA extraction. RNA was extracted following a modified TRIzol
413 (Invitrogen Cat. No. 15596026) protocol, purified using the Invitrogen PureLink® RNA Mini Kit
414 (Thermo Cat. No. 12183025) and treated twice with DNase. See supplemental methods for
415 more details.
416
417 RNA sequencing and analysis

418 Full details for RNA sequencing and analysis can be found in the supplemental methods.
419 Briefly, once RNA was purified and satisfied quality control measures, we performed ribosomal
420 RNA depletion using the RiBO-COP rRNA Depletion Kit for Gram-Negative Bacteria (Lexogen
421 Cat. No. 126.96). Library generation was done using Lexogen RNA sequencing kits, following
422 manufacturers protocols. Sequencing was performed in house on an Illumina NextSeq550 with
423 the corresponding High-Output Kit v2.5 75 cycles (Illumina 20024906). Raw reads are uploaded
424 to the NCBI BioProject ID PRJNA1214285. Reads were assessed for quality, processed, and
425 aligned to the reference genomes using kallisto (73). This analysis provided the gene abundance
426 metrics, measured in transcripts per million transcripts (TPM), which normalizes by both gene
427 length and sequencing depth. Differential expression analysis was done with DESeq2 (74).
428 Unless otherwise stated, cutoffs for significance were set to a false discovery rate adjusted p-
429 value < 0.05 and a magnitude of $\log_2$FoldChange > 1. RNA sequencing performed on three
430 biological replicates for each sample by treatment combination except for removal of two
431 replicates due to low sequencing coverage or outlier status (17978UN population 1 untreated
432 replicate A and AB5075-UW population 2 untreated replicate C), and averages of the replicates
433 are presented.
434
435 Experimental evolution with TGC
436 Our experimental design was adapted from previous studies (47, 51). Lineages were
437 inoculated from overnight culture with a 1:100 dilution into fresh media with or without TGC,
438 resulting in approx. 6.6 generations per day (75). The experiment was designed such that the
439 populations were not mutation limited (see supplemental methods). In the TGC treated
440 condition, the TGC level in the media was tailored to the initial susceptibility level of each
441 strain, starting at 0.5x the ancestral MIC (subinhibitory). Every three days, the concentration of
442 TGC in the media was doubled (Fig. S5). We propagated the lineages for 12 days, with the final
443 TGC media concentration at 4x the ancestral MIC, which crossed the clinical breakpoint for
444 resistance in both strains. Populations were periodically sampled and frozen in 9% DMSO at -
445 80°C, as well as pelleted and frozen at -20°C for DNA extraction.
446
447 Whole-population, whole-genome sequencing, and analysis
448 DNA was extracted from frozen cell pellets using the DNeasy blood and tissue kit for the
449 QIAcube (Qiagen, Hilden, Germany) with a 10-minute elution into nuclease-free water. Libraries
450 were prepared in-house as previously described (76) or using the plexWell™ kit following
451 manufacturer's directions (SeqWell PW096). Libraries were sequenced using an Illumina
452 NextSeq550 sequencer with a 300 cycle mid-output kit (Illumina 20024905). Raw reads are
453 uploaded to the NCBI BioProject ID PRJNA1214285. Reads were demultiplexed, trimmed, and
454 quality checked as described in the supplemental methods for the RNAseq reads. Breseq
455 (v0.35.0) was used for read mapping and variant calling (77) with subsequent filtering following

456 previously published rationale (51) with special attention to new junction calls. Filtering,
457 consolidating for allele frequencies, and plotting were done in RStudio (R v4.2.1) with the
458 packages ggplot2 (v3.4.2; https://CRAN.R-project.org/package=ggplot2) and tidyr (v1.3.0;
459 https://CRAN.R-project.org/package=tidyr).
460
461 Growth curves as measure of fitness
462 We use bacterial growth curves to measure absolute fitness of ancestral clonal samples
463 as well as to measure aggregate absolute fitness of evolved populations (78). Growth curves
464 were seeded to mimic the transfers of the evolution experiment. A large sample of the frozen
465 population (or ancestor) stock was inoculated, in biological triplicate, into M9plus media and
466 grown for 24h. Overnight cultures were then diluted 1:100 into fresh media and OD600
467 measured every 10 minutes for 24h. Fitness was measured, in technical triplicate, in plain
468 M9plus as well as in M9plus containing 0.06 µg/mL TGC. We use area under the curve (AUC) to
469 measure fitness of populations normalized by the AUC of their respective ancestor ($AUC_{evolved}$
470 $_{population}$/$AUC_{ancestor\ average}$). Analyses were done in RStudio (R v4.2.1) utilizing previously
471 published pipelines (79) (https://github.com/mjfritz/Growth_Curves_in_R).
472
473 Measurements of efflux expression and activity
474 Efflux activity of late exponential phase cultures was assessed using the ethidium
475 bromide efflux activity assay. Fluorescence intensity was measured at three minutes post
476 addition of ethidium bromide to washed cells with an excitation of 530 nm and emission of 600
477 nm. Quantitative reverse transcriptive PCR was used to measure expression of efflux pump
478 components. RNA extraction was done as previously described (supplemental methods). The
479 Power SYBR Green RNA-to-Ct 1-Step Kit (Applied Biosystems) was used for cDNA synthesis and
480 qPCR with custom primers (Table S2). Data were analyzed for ΔCt and ΔΔCt, normalized by rpoB
481 and ancestor, respectively, within strain background. Expression values are presented as 2^{-}
482 $^{normalized\ expression}$ such that higher values indicate increased expression. We used the main efflux
483 pump gene (adeB, G, and J) as a representative for pump expression (57, 80). More information
484 on assays of efflux activity and expression can be found in supplemental methods.
485
486 **ACKNOWLEDGEMENTS**
487 We thank all members of the Cooper Lab as well as our collaborators in the Combating
488 Antibiotic-Resistant Bacteria Interdisciplinary Research Units (NIH CARBIRU) for thoughtful
489 discussions and feedback. We are especially grateful for bioinformatic guidance from Emma G.
490 Mills and Nanami Kubota. We thank Michelle R. Scribner for direction on the initial project
491 design and assistance in uploading data to the NCBI BioProject. This work was supported by NIH
492 U19AI158076 and, in part, by PA CURES Grant #4100085725. ABR is also supported by NIH
493 1F31AI172279-01A1 as well as a Catalyst Award from the Pittsburgh Center for Evolutionary

494 Biology and Medicine (CEBaM). ASL is currently supported by the Ministry of Science,
495 Innovation and Universities through a Ramon y Cajal fellowship (RYC2022-037765-I).
496
497

498 **FIGURES**
499

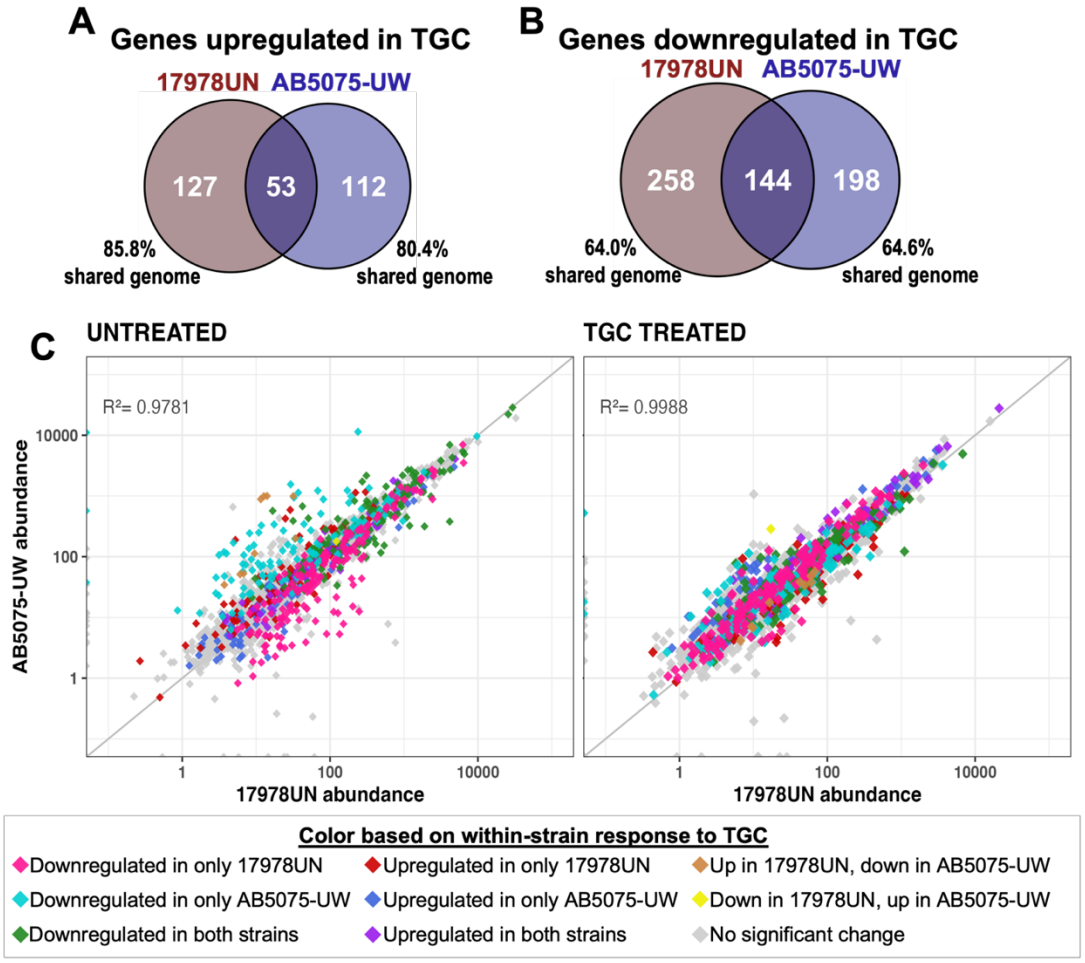

500
501

502 **Fig. 1: Transcriptional response to TGC is highly strain dependent and results in a shift toward**
503 **a more conserved transcriptional state.** Counts of differentially expressed genes, upregulated
504 (*A*) or downregulated (*B*), in each strain in response to TGC treatment. Overlapping regions
505 represent genes that were similarly differentially expressed in both strains. Percentage of genes
506 that were significantly differentially expressed in one strain but are still encoded by both strains
507 (shared genome) is indicated, showing minimal involvement of accessory genes. (*C*) Each point
508 represents the abundance of one gene in each strain in that condition (left: untreated plain
509 M9plus media; right: TGC treated with 0.06 µg/mL TGC). Diagonal y = x line represents equal
510 gene abundance in both strains and R^2 linear regression fits to this line are indicated. Points are
511 colored based on within-strain significant differential expression upon TGC treatment. See
512 Animation S1 for an animation of these transcriptional responses, and Fig. S4 for accessory
513 gene transcriptomic responses and a version of this plot with colors separated.
514

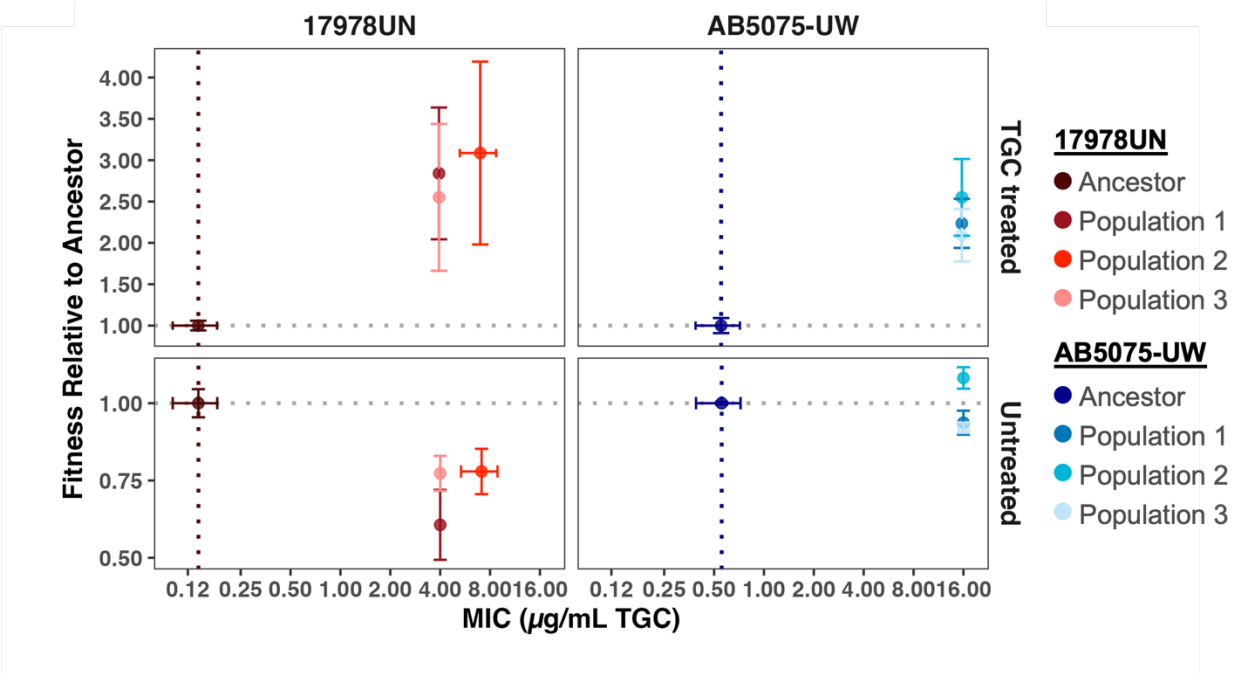

Fig. 2: Strain specific patterns in fitness-resistance tradeoffs. Minimum inhibitory concentration (MIC) to TGC was measured for ancestors and for day-12 TGC-evolved populations. Relative fitness was calculated from growth curves as described in the methods. Fitness of 1.00 (gray horizontal dotted line) indicates the population grew equally well to its respective ancestor in that environment (untreated M9plus or TGC treatment at 0.06 µg/mL TGC). Points represent mean across replicates and error bars show standard deviation of the mean.

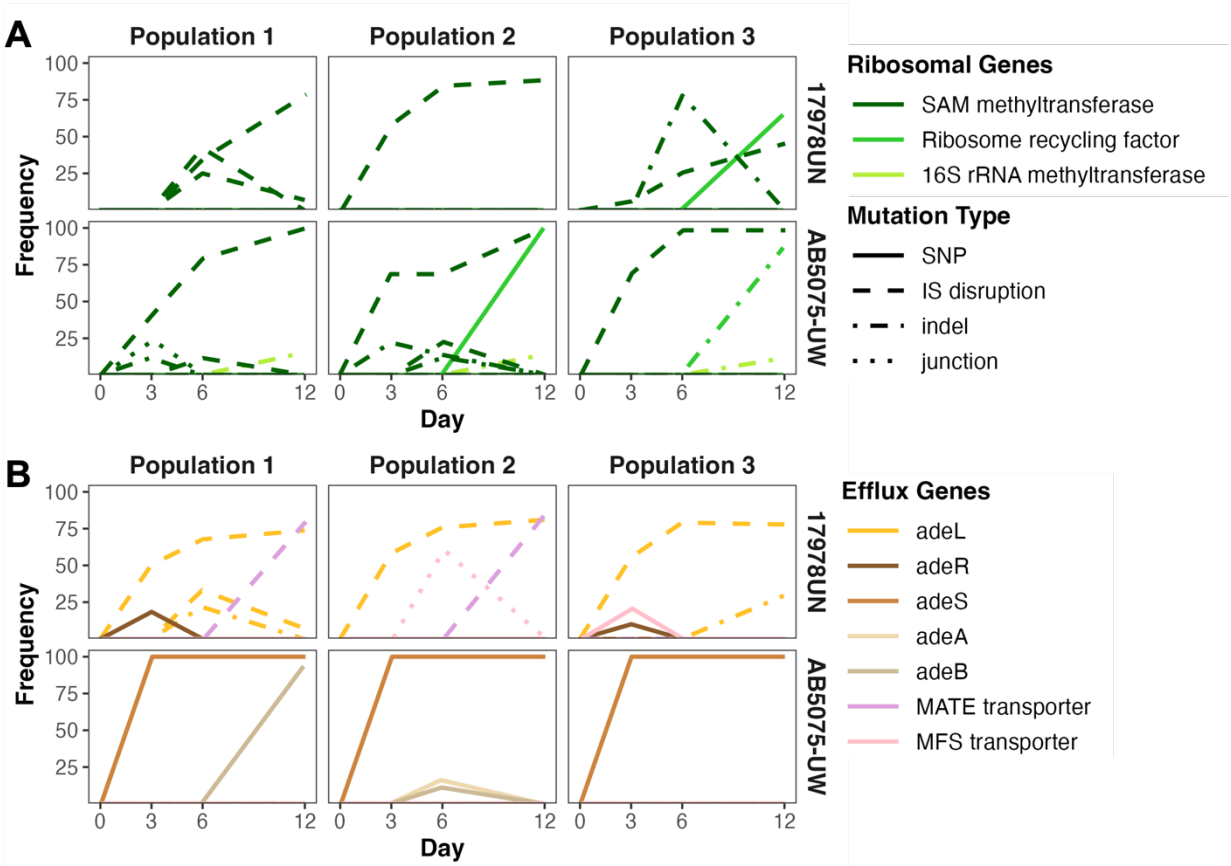

Fig. 3: Whole-population genome sequencing reveals similar resistance mechanisms but different population dynamics between strains. Evolved mutation frequencies over time, with line colors corresponding to affected gene and line patterns indicating mutation type. Abbreviations: SNP = single nucleotide polymorphism; IS = insertion sequence, indel = insertion or deletion, and junction = structural variant indicated by a new junction call. Multiple lines of the same color indicate more than one unique mutation arose in that gene. (*A*) Mutations in genes associated with the ribosome. (*B*) Mutations in genes associated with efflux pumps.

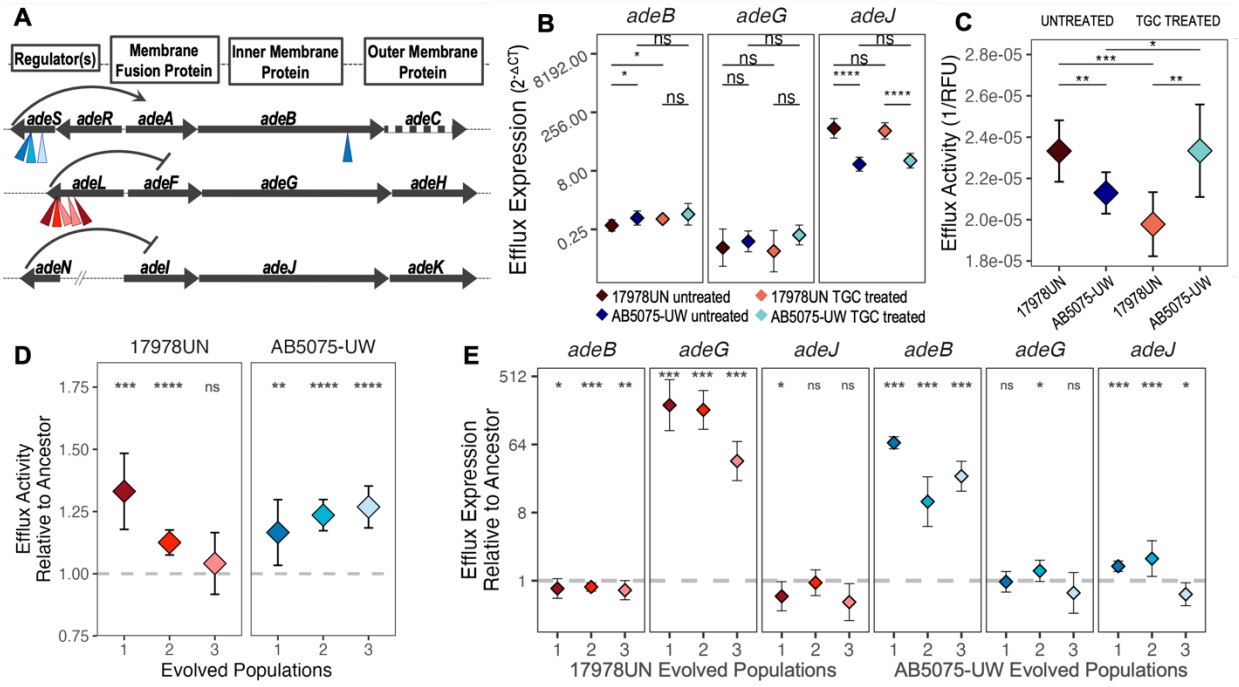

Fig. 4: Genetic distinctions of evolved efflux expression and activity (*A*) Representation of the RND efflux pump operons/regulators. All RND genes are highly conserved between the two strains (supplemental table 2), except that 17978UN does not encode *adeC.* Arrow size is scaled to the length of the gene. Inverted triangles depict mutations present on day 12, colored by the population in which they are found. Ancestral efflux activity (*B*) and expression (*C*) in treated (0.06 µg/mL TGC) or untreated states. (*D*) Efflux activity of the evolved populations when grown in the untreated state relative to respective ancestor. (*E*) Efflux expression in evolved populations normalized by the respective untreated ancestor. Points represent mean and error bars depict standard deviation. Statistically significant differences were determined with t-tests in B and C with the comparisons depicted by lines, and with Wilcoxon tests compared to an ancestral value set at 1 in D and E. Significance criteria: ns for $p > 0.05$, * for $p \leq 0.05$, ** for $p \leq 0.01$, *** for $p \leq 0.001$, and **** for $p \leq 0.0001$.

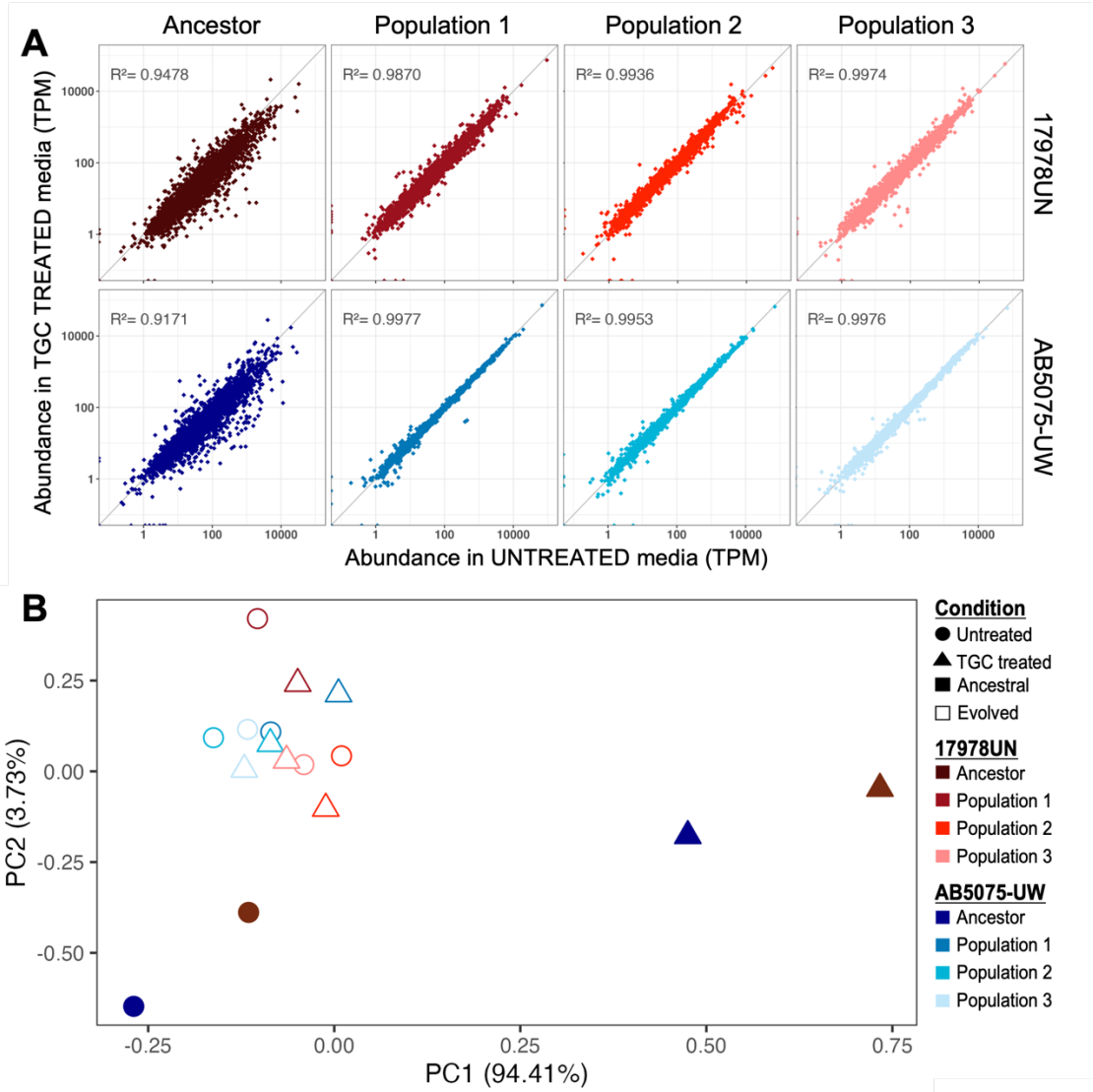

Fig. 5: Transcriptional response evolves to minimally react to TGC pressure. (*A*) Conserved transcript abundance regardless of TGC treatment in all evolved populations. Each point represents the abundance of one gene in each sample. Point position depicts expression in each condition (untreated M9plus, or 0.06 µg/mL TGC). Top row shows ancestor and TGC-evolved populations for 17978UN, and the bottom row is the same for AB5075-UW. Diagonal y = x line represents equal gene abundance in both conditions and R^2 linear regression fits to this line are indicated. (*B*) Principal component analysis showing that ancestral transcriptomes are strain dependent, but TGC treatment produces a conserved shift. Evolved population transcriptional adaptation is conserved between strains and indifferent to TGC treatment. Point color indicates sample, shape indicates culture condition either untreated or 0.06 µg/mL TGC treated, fill indicates either ancestral or evolved populations.

563 **SUPPLEMENTAL ANIMATION**

564

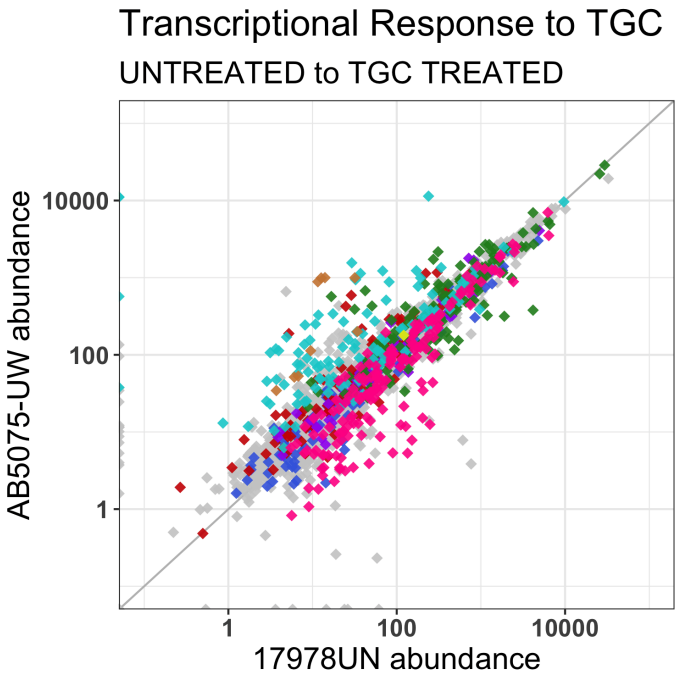

565

566 **Animation S1: Tigecycline treatment induces a shift toward a more conserved transcriptional**
567 **response.** Animation of main text figure 1, showing movement of genes from the untreated
568 state to the TGC treated state. See figure 1 for color key and legend.

569

570

571 **SUPPLEMENTAL FIGURES**

572

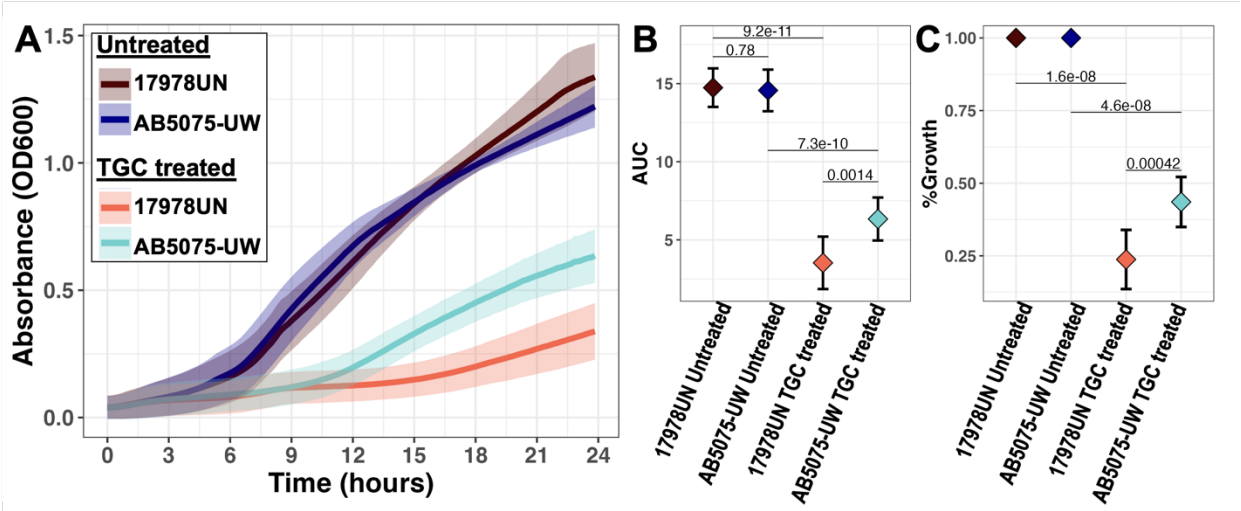

573

574 **Fig. S1: Ancestral growth in treatment conditions.** Growth was measured in minimal M9plus
575 media (Untreated) or M9plus with addition of 0.06 µg/mL TGC (TGC treated) with three
576 biological replicates (batches), each with three technical replicates. (*A*) Growth curves for
577 ancestors grown in different conditions. Solid line represents mean, and ribbons depict
578 standard deviation. (*B*) Area under the curve (AUC) quantifications of curves in A (used to
579 normalize evolved population growth in Fig. 2). (*C*) Treatment effect on ancestral growth. Y-axis
580 shows the percent growth defect caused by TGC treatment on each strain, normalized by
581 within-batch growth in plain media. For B and C, mean and standard deviation depicted by
582 point and error bars, p-values calculated from pairwise t-test.

583

584

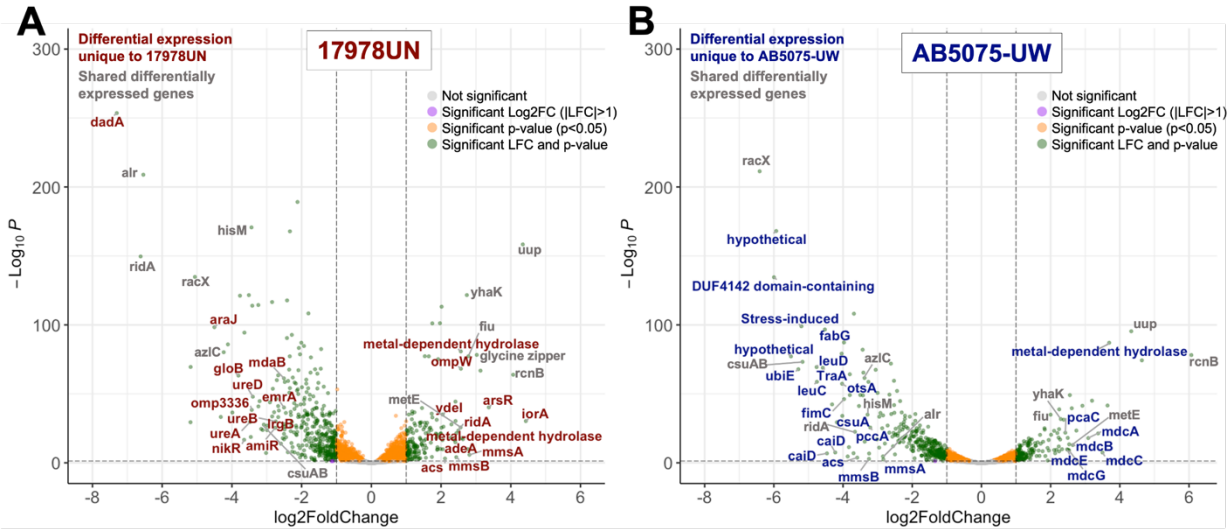

Fig. S2: Transcriptional response to TGC is strain dependent. Volcano plots of differential expression in 17978UN (*A*) and AB5075-UW (*B*). Points are colored based on significance status and fold change; Labels are colored based on if the gene is significantly differentially expressed in only 17978UN (red), in only AB5075-UW (blue), or significant in both strains (gray). Labels were manually curated to label the strongest hits or hits that showcase differences between the strains. RNAseq was done in triplicate for each strain x treatment. Genes were included as significant in the counts/plots if they had an absolute value of log 2-fold change > 1 and a p-value ≤ 0.05.

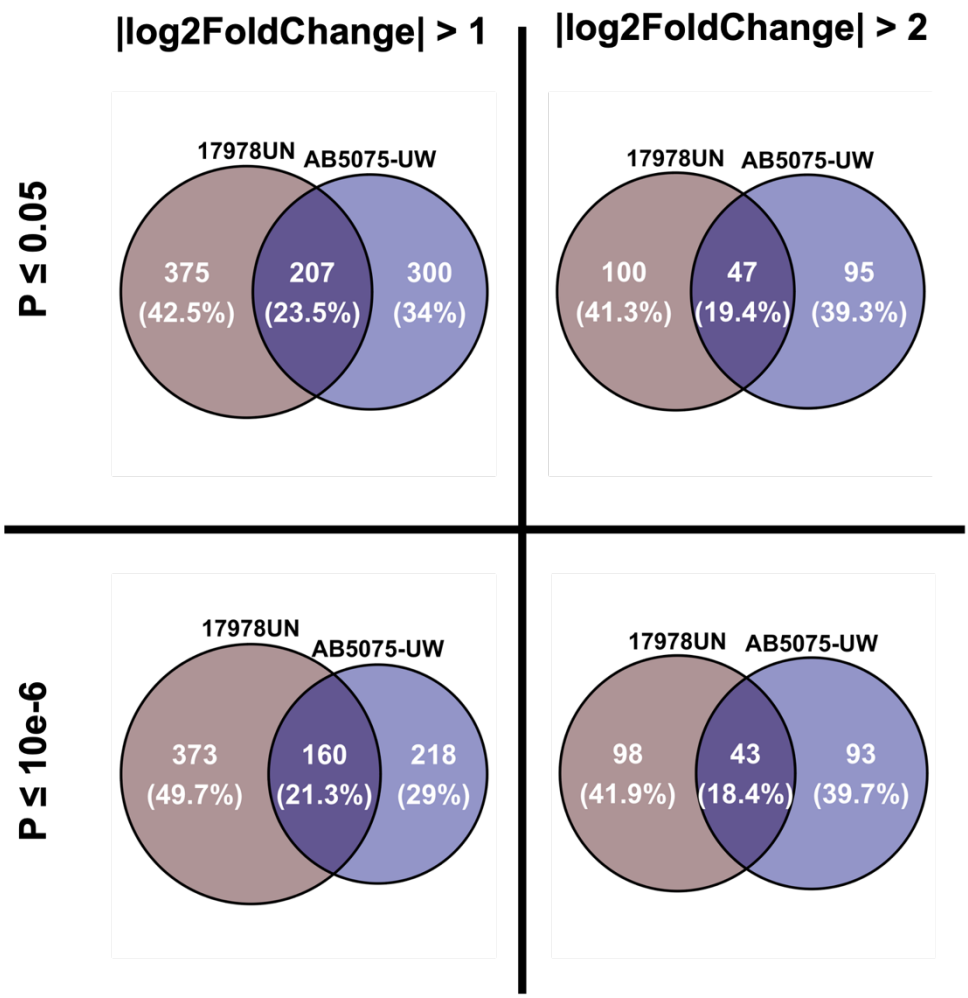

Fig. S3: Significance cut-off criteria does not affect amount of differential expression overlap between strains. All differentially expressed genes (both upregulated and downregulated) in response to TGC treatment were summed. Varying cut-offs for calling significance in p-value and in log 2-fold change were tested to determine if the patterns of differential expression overlap between strains would differ. The overlap in differentially expressed genes between strains slightly decreases as increasingly strict significance criteria are applied.

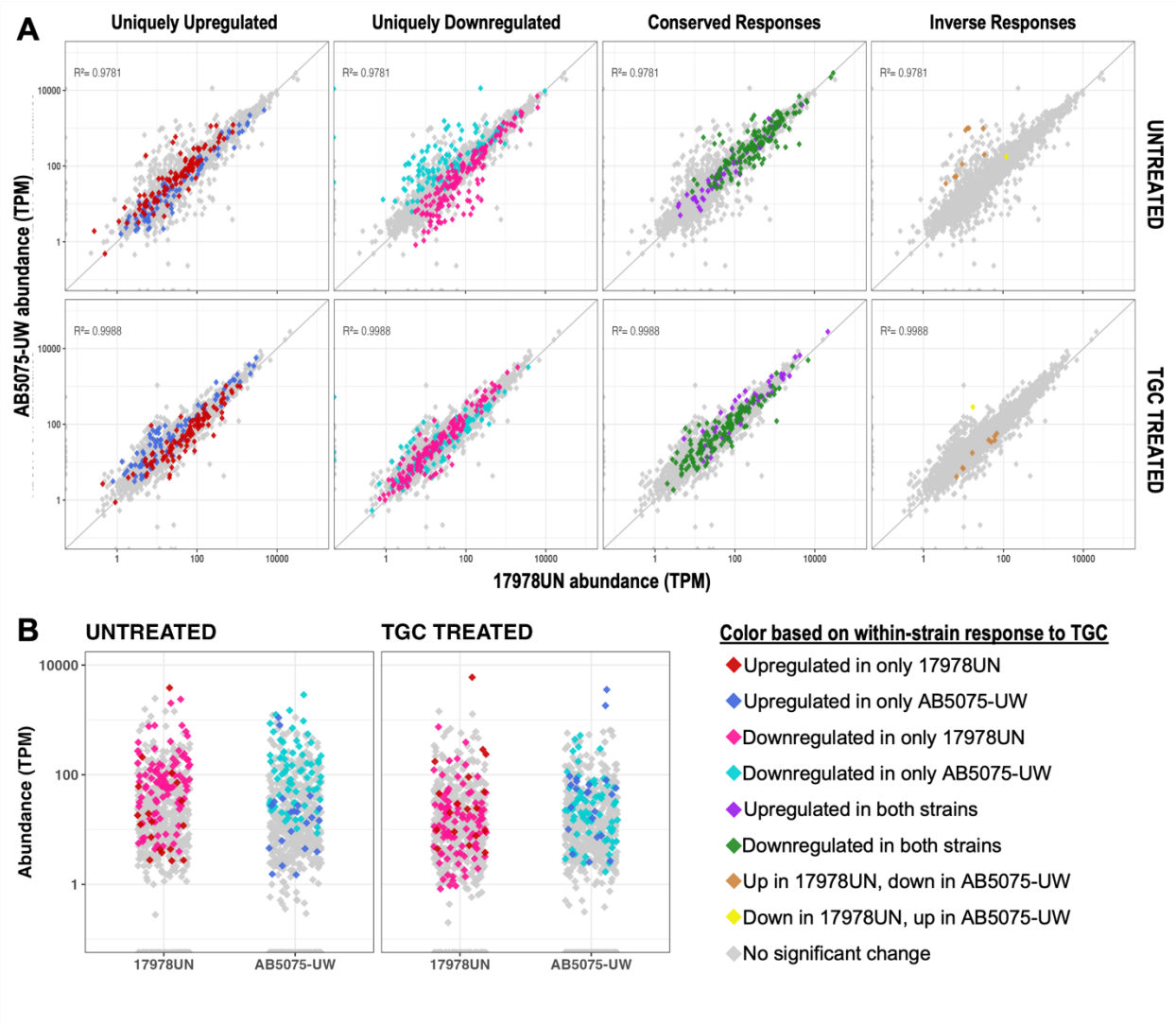

Fig. S4: Strain-dependent transcriptional response to TGC results in a shift toward a more conserved transcriptional state. (*A*) Specific directional gene responses with genes colored based on how that gene responds within-strain upon TGC pressure. The top panels show gene abundances in untreated media and bottom panels show gene abundance in TGC treatment (0.06 µg/mL). Only genes falling under the bin of directional response noted above the plots are colored. All other genes, even those with significant TGC responses, are gray in these plots. (*B*) Abundance plots of the accessory genes, using the same colors as in A and in main text figure 1. See figure 1 legend for more details.

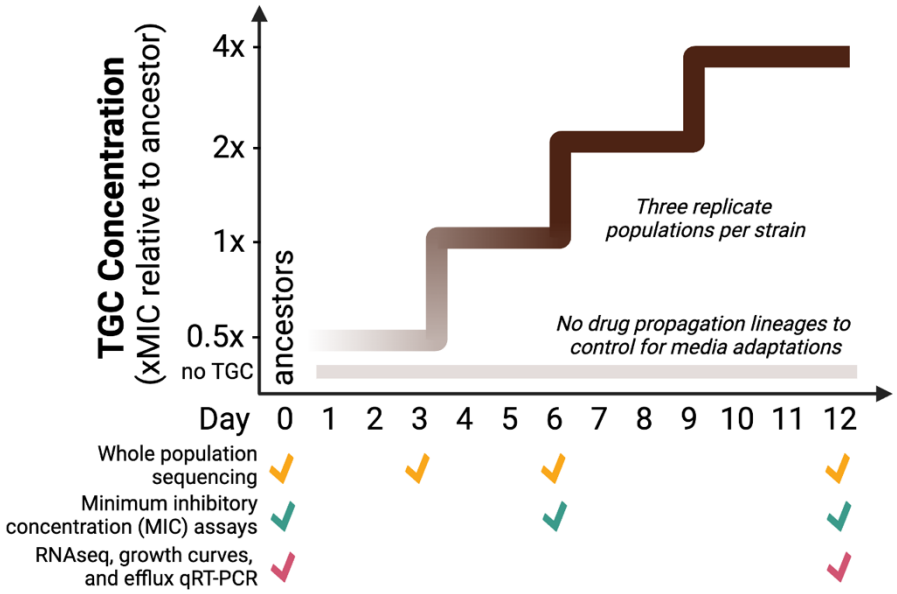

Fig. S5: Experimental design and post-experiment assay timings. Schematic for the design of the experimental evolution. For in-depth design, see the methods section. Bottom panels highlight when various phenotype/genotype assays were performed. Dark steps indicate TGC concentration doubling every three days of the experiment. Faint bar on bottom represents lineages propagated in M9plus media lacking antibiotic to assess media adaptations.

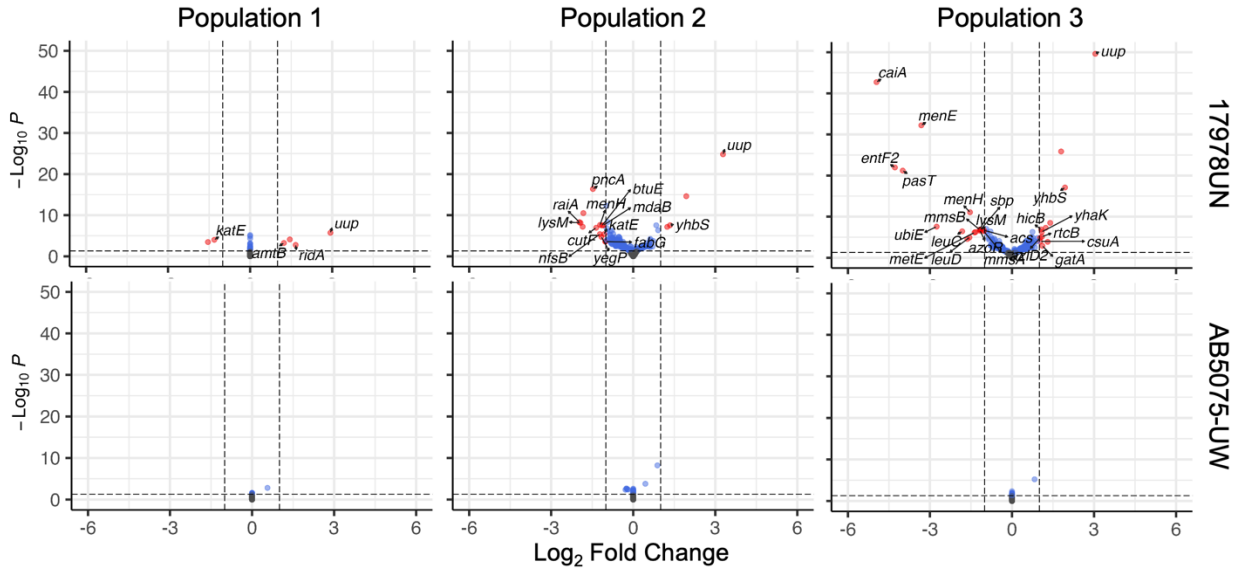

Fig. S6: Transcriptional response to TGC in evolved populations is minimal, especially in lineages of AB5075-UW. A handful of genes significantly respond to TGC treatment (0.06 µg/mL), compared to growth in untreated media, in evolved populations of 17978UN (*top*), but no genes significantly respond to TGC in any evolved population of AB5075-UW (*bottom*). All samples are from day 12 of the TGC evolution experiment. Data is from averages of three biological replicates for all sample x treatment combinations except for removal of two replicates due to low sequencing coverage or outlier status (17978UN population 1 untreated replicate A and AB5075-UW population 2 untreated replicate C). Differential expression significance cutoffs: |LFC|>1 and p-value ≤ 0.05.

636 **SUPPLEMENTAL TABLES**
637 Tables S1-S4 can also be found at https://github.com/vscooper/tigecycline
638
639 **Table S1: Genomic comparisons between strains.** Summary of strain similarities and
640 differences in various genomic categorizations, including gene count in clusters of orthologous
641 group (COG) categories, total genes assigned COG categories, AMR finder found resistance
642 elements, and annotated insertion sequences. A proportional z-test was performed for all
643 appropriate comparisons with the relevant gene count as the proportion denominator.

		AB5075-UW	17978UN	p-value (proportional z-test)
COG Categories	Cell cycle control, cell division, chromosome partitioning	34	37	1
	Cell motility	40	44	1
	Cell wall, membrane and envelope biogenesis	170	188	0.957
	Cytoskeleton	2	2	1
	Defense mechanisms	61	75	0.547
	Extracellular structures	36	39	1
	Intracellular trafficking, secretion, and vesicular transport	58	60	0.832
	Posttranslational modification, protein turnover, chaperones	115	128	0.94
	Signal transduction mechanisms	108	122	0.855
	Replication, recombination and repair	87	104	0.583
	RNA processing and modification	1	2	1
	Transcription	251	287	0.619
	Translation, ribosomal structure and biogenesis	217	224	0.561
	Amino acid transport and metabolism	276	278	0.33
	Carbohydrate transport and metabolism	126	126	0.508
	Coenzyme transport and metabolism	155	170	1
	Energy production and conversion	164	170	0.654
	Inorganic ion transport and metabolism	165	191	0.619
	Lipid transport and metabolism	197	219	0.902
	Nucleotide transport and metabolism	84	84	0.61
	Secondary metabolites biosynthesis, transport and catabolism	55	68	0.553
	Function unknown	113	130	0.736
	General function prediction only	210	232	0.951
	Total number of genes with COG assignments	2725	2980	**1.55E-12**
	AMRfinder Plus found elements	19	6	**0.017**
	Annotated IS elements	14	14	1

644
645
646
647
648
649
650
651
652
653
654
655
656
657

Antibiotic	17978UN	AB5075-UW
Amikacin	≤ 8 µg/mL S	32 µg/mL I
Ampicillin	≤ 4 µg/mL S	> 32 µg/mL R
Ampicillin/sulbactam	≤ 4/2 µg/mL S	16/8 µg/mL I
Aztreonam	16 µg/mL I	> 32 µg/mL R
Cefazolin	> 32 µg/mL R	> 32 µg/mL R
Cefepime	≤ 4 µg/mL S	> 32 µg/mL R
Cephalothin	> 16 µg/mL R	> 16 µg/mL R
Meropenem	≤ 1 µg/mL S	> 8 µg/mL R
Ertapenem	≤ 2 µg/mL S	> 16 µg/mL R
Cefuroxime	16 µg/mL R	> 32 µg/mL R
Gentamicin	≤ 2 µg/mL S	≤ 2 µg/mL S
Ciprofloxacin	≤ 0.5 µg/mL S	> 4 µg/mL R
Piperacillin / tazobactam	≤ 16/4 µg/mL S	> 128/4 µg/mL R
Cefoxitin	32 µg/mL R	> 32 µg/mL R
Trimethoprim / sulfamethoxazole	> 4/76 µg/mL R	≤ 0.5/9.5 µg/mL S
Cefpodoxime	4 µg/mL I	> 16 µg/mL R
Ceftazidime	2 µg/mL S	4 µg/mL S
Tobramycin	≤ 4 µg/mL S	≤ 4 µg/mL S
Tigecycline*	**≤ 1 µg/mL** **S**	**≤ 1 µg/mL** **S**
Ticarcillin / clavulanic acid	≤ 16/2 µg/mL S	> 64/2 µg/mL R
Ceftriaxone	8 µg/mL I	16 µg/mL I
Tetracycline	≤ 0.5 µg/mL S	≤ 0.5 µg/mL S

Table S2: Resistance profiles for the laboratory reference strain, 17978UN, and the multi-drug resistant clinical reference strain, AB5075-UW. Susceptibility/resistance state was measured in duplicate for each strain to a variety of Gram-negative acting antibiotics via Sensititre plates #GN3F (ThermoFisher). Sensitive (S), intermediate (I), and Resistant (R) classifications were assigned using CLSI standards for Gram-negative bacteria. *Tigecycline was chosen for further use in this study and broth-dilution MICs were determined to differ 1-fold between the strains.

Protein	Length	Amino Acid Pairwise Identity (%)
AdeS	362	97.2
AdeR	248	100
AdeA	397	98.7
AdeB	1037	99.5
AdeC	466	*
AdeN	218	100
AdeI	417	100
AdeJ	1059	99.9
AdeK	485	100
AdeL	344	99.7
AdeF	407	99.5
AdeG	1060	99.9
AdeH	483	99.8

Table S3: Conservation of efflux proteins between 17978UN and AB5075-UW. Pairwise identity of amino acid sequences. * *adeC* is only encoded by AB5075-UW, but it is suggested that *adeK* can assume the function of *adeC* in 17978UN (Leus et. al., 2018). Importantly, all sites that will be mutated upon TGC adaptation are initially identical between the strains.

716

717 **Table S4: List of primers used for Q-RT-PCR.** Quantative, reverse-transcriptase PCR was
718 performed on the inner membrane pump of the three RND efflux pumps as documented in the
719 methods using primers with the characteristics listed here. The housekeeping gene *rpoB* was
720 used as a control.

Target	Direction	Sequence (5'-3')	Melt Temp (ºC)	Product Size	Source
rpoB	forward	TCCGCACGTAAAGTAGGAAC	57.6	155	Coyne et al. Antimicrobial Agents and Chemotherapy
	reverse	ATGCCGCCTGAAAAAGTAAC	57		
adeB	forward	AAAGGTATTGGCTACGAGTGG	57.7	132	Lin et al. Frontiers in Microbiology. 2017
	reverse	TGCCCAGCTTTCATAGAGTG	57.6		
adeG	forward	CAAAGTCCAGCATTACCAGC	57.1	136	This study, geneious primer3
	reverse	CTGCCCCAGGTTATTCATCT	57		
adeJ	forward	TGACCAACACCTGTGAATGA	57	164	This study, geneious primer3
	reverse	GAAGATCAGGGTGTGGTCAT	56.9		

721
722
723 **SUPPLEMENTAL DATA LEGENDS**
724 *There are three submissions for supplemental data, each a separate file that can be accessed*
725 *through* https://github.com/vscooper/tigecycline
726 *Please contact authors for additional information about supplemental data.*
727 **Data S1: Ancestral gene annotations and RNA sequencing results.**
728 **Data S2: Filtered results of whole-population, whole-genome sequencing throughout the**
729 **evolution experiment.**
730 **Data S3: RNA sequencing results of the evolved populations.**
731
732

733 **SUPPLEMENTAL METHODS**

734 *Supplemental methods citations found after main text citations.*

735 Bacterial strains and growth conditions

736 Laboratory reference strain ATCC 17978UN (1, 2) and clinical reference strain AB5075-
737 UW (3, 4) were used throughout the study and grown under the same conditions. Unless
738 otherwise stated, bacterial cultures were grown in 5ml M9+ media, as previously described (5).
739 Briefly, M9+ media is a salts-buffered media with glucose (11.1mM) as the primary carbon
740 source. It contains 0.1 mM $CaCl_2$, 1 mM $MgSO_4$, 42.2 mM Na_2HPO_4, 22 mM KH2PO_4, 21.7 mM
741 NaCl, 18.7 mM NH_4Cl and is supplemented with 20 mL/L MEM essential amino acids (Gibco
742 11130051), 10 mL/L MEM nonessential amino acids (Gibco 11140050), and 1 mL each of trace
743 mineral solutions A, B, and C (Corning 25021–3 Cl). Cultures were incubated at 37°C with
744 shaking or on a roller-drum at approximately 250rpm.

745

746 Genomic comparison of the two strains

747 Genomes were annotated with bakta (v1.6.1, database v4.0) (6) and input to Panaroo
748 (v1.3) in the sensitive clean mode to obtain a gene presence/absence list that included plasmid
749 encoded genes (Data S1) (7). We assessed pairwise nucleotide similarity of the two strains with
750 pyANI (v0.2.12; (8). Multilocus sequence types were confirmed using mlst (v2.11;
751 https://github.com/tseemann/mlst) (9). Elements associated with resistance, including known
752 single nucleotide polymorphisms (SNPs), were detected with AMRfinderPlus (version 3.11.26
753 with database version 2023-11-15) (10). Two-proportion z-tests on two-tailed hypotheses were
754 used to determine if gene content in clusters of orthologous group (COGs) categories was
755 significantly different in the two strains, accounting for the difference in genome size (Table S1)
756 (11). The annotated reference genomes used in this study can be found in the NCBI BioProject
757 ID PRJNA1214285.

758

759 Measuring resistance

760 Broad resistance profiles of the two strains were determined using Sensititre plates
761 (ThermoFisher, GN3F), commercially available panels of 23 antibiotics relevant to Gram-
762 negative pathogens at dilutions spanning the clinical breakpoint for resistance as set by the
763 Clinical and Laboratory Standards Institute (CLSI) (12). Broth microdilution and inoculation of
764 the plates was performed following the manufacturer's instructions. Sensititre plates were
765 performed in biological triplicate for each strain.

766 Minimum inhibitory concentration (MIC) assays were performed to measure
767 susceptibility levels more accurately to tigecycline (TGC, Sigma 220620-09-7). MIC assays were
768 performed following modified CLSI methods (12). MIC results presented here are from MIC
769 assays performed in M9plus media. Reference MIC assays were performed in the standard
770 Mueller Hinton broth and showed little-to-no (maximum difference of 1-fold) difference to

771 those performed in M9plus media. Biological triplicate (multiple samples from the frozen
772 ancestors or populations) with technical triplicates for each assay were performed. We present
773 the concentration of antibiotic that inhibits 90% growth (IC_{90}), measured via optical density at
774 600nm, as the MIC for each antibiotic.
775
776 RNA extraction and purification
777 For transcriptome analysis of the ancestor strains, cultures were seeded from individual
778 colonies in biological triplicate into 5mL M9plus media. Population cultures were started
779 directly by inoculating a large sampling of freezer stock into 5mL M9plus, also in triplicate. All
780 cultures were grown over-night at 37°C and back diluted 1:100 into 25 mL pre-warmed M9plus
781 with or without 0.06 µg/mL TGC. In this way, each biological replicate over-night culture results
782 in a paired set of treated and untreated TGC culture for analysis, thus limiting the effect of
783 sampling bias for the populations. Cultures were grown until reaching mid-log phase (OD600 =
784 0.6 +/- 0.05), at which time cultures were pelleted, resuspended in TRIzol (Invitrogen Cat. No.
785 15596026) and stored at -80°C for subsequent extraction and purification.
786 RNA was extracted following a modified protocol (13) for TRIzol extraction with
787 purification using the Invitrogen PureLink® RNA Mini Kit. Extraction included one bead beating
788 step followed by TRIzol-chloroform extraction with ethanol precipitation. Purification was done
789 using RNA columns from the Invitrogen PureLink system with final elution into nuclease free
790 water. RNA samples were treated with DNase 1 off-column with additional DNase spike-in
791 during incubation (NEB DNase and buffer Cat. No. M0303S) as well as treated with DNase 1 on-
792 column (Qiagen Cat. No. 79254) during final purification steps on the Invitrogen columns. RNA
793 concentration and quality were assessed using nanodrop (all 260/280 ratios > 2). Pure RNA was
794 stored at -20°C for less than a week prior to library preparation and at -80°C for longer-term
795 storage. Step-by-step RNA protocols are available upon request.
796
797 RNA sequencing and analysis
798 RNA integrity, fragment distribution, and RIN^e scores were assessed on Tapestation
799 using the High Sensitivity RNA ScreenTape, sample buffer, and ladder from Agilent Technologies
800 (Part Numbers: 5067 -5579, -5580, -5581). All RIN^e scores satisfied subsequent ribo-depeletion
801 requirements for quality (the majority of RIN^e scores were >8). rRNA depletion was performed
802 using the RiBO-COP rRNA Depletion Kit for Gram-Negative Bacteria (Lexogen Cat. No. 126.96)
803 and directly following the manufacturer's protocols with an initial RNA input of approximately
804 200ng. RNA libraries including ancestral strain RNAs were prepared using the CORALL Total
805 RNA-Seq Library Prep Kit (Lexogen Cat. No. 095) while the evolved populations were sequenced
806 with the RNA-Seq V2 Library Prep Kit with UDIs (Lexogen Cat. No. 171.96). Both library
807 preparations included the PCR add-on step to determine ideal cycle number (11 cycles) for
808 library amplification (Lexogen Cat. No. 020). The uniquely indexed samples for each library were

809 pooled based on fragment size and concentration and the pool was diluted to 4nM for
810 sequencing. Each library was denatured and loaded at a final concentration of 2pM with a 5%
811 phiX spike-in. Sequencing was performed on the Illumina NextSeq550 with the corresponding
812 High-Output Kit v2.5 75 cycles (Illumina 20024906). Raw reads are uploaded to the NCBI
813 BioProject ID PRJNA1214285.
814 Reads were demultiplexed using bcl2fastq (v2.17.1) and trimmed with trimmomatic
815 (v0.36, custom criteria as follows: LEADING:3 TRAILING:3 SLIDINGWINDOW:4:15 MINLEN:36).
816 Read quality was confirmed with fastQC (v0.11.5) and kallisto (v0.48.0, flags as follows: --single
817 -l 315 -s 26) was used for pseudoalignment with custom made index files from the
818 concatenated bakta annotated fasta files previously described for each reference strain (14).
819 Sequencing coverage was satisfactory (>10^7 reads/sample, resulting in >200x coverage) for all
820 samples apart from one replicate of AB5075-UW evolved population 2 in the untreated
821 condition, which had unusually low coverage and was removed from further analysis. We also
822 removed one replicate of 17978UN evolved population 1 in the untreated condition. DESeq2
823 (v1.38.3; (15)) was used in RStudio (R v4.2.1) for differential expression analysis supplemented
824 with EnhancedVolcano (v1.16.0) for plotting. Transcript abundance is reported as transcripts
825 per million transcripts (TPM) which normalizes by both gene length and sequencing depth. TGC
826 imposed differential expression analyses were performed with guidance from established
827 tutorials (15, 16). In the results function for analysis of the DESeq Data Set, we specified to turn
828 off independent filtering and cooksCutoff to keep outliers and calls with low coverage in the
829 analyses, then the apeglm method was applied for log fold change shrinkage (17). Unless
830 otherwise stated, cutoffs for significance were set to a false discovery rate adjusted p-value <
831 0.05, with the Benjamini and Hochberg correction for multiple comparisons, and a magnitude
832 of $\log_2$FoldChange > 1.
833
834 <u>Experimental evolution with TGC</u>
835 Our experimental design was adapted from previous studies (5, 18). Both strains were
836 resurrected from the freezer via streaking on LB agar plates. A single colony of each strain was
837 used to inoculate a 5mL overnight culture in M9+. After approximately 18 hours, the saturated
838 culture was used to inoculate multiple independent lineages for the evolution experiment. We
839 propagated five replicate lineages of each strain in each condition, either with or without TGC.
840 Lineages were inoculated from overnight culture (either the starting overnight, or the prior day)
841 with a 1:100 dilution into fresh media with or without TGC. 1:100 dilutions from saturated
842 overnight cultures results in approximately 6.6 generations per day (19). The large population
843 size combined with the 1% bottleneck, mutation rate, and doubling time of *A. baumannii*
844 provides a large mutation supply, with a probability >1 that each site can see a mutation (19).
845 Lineages were propagated in the presence and absence of TGC, resulting in two
846 conditions. The no drug lineages were used to control for adaptations to the media and

847 experimental conditions. In the TGC treated condition, the TGC level in the media was tailored
848 to the initial susceptibility level of each strain, starting at 0.5x the ancestral MIC (subinhibitory).
849 Every three days, the concentration of TGC in the media was doubled (Fig. S5). We propagated
850 the lineages for 12 days, with the final TGC media concentration at 4x the ancestral MIC, which
851 crossed the clinical breakpoint for resistance in both strains. On days 0, 1, 3, 4, 6, 7, 9, 10, 12,
852 corresponding to days before and after antibiotic level increases, the populations were stocked
853 for later assays and sequencing (frozen in 9% DMSO at -80°C, and a cell pellet from 1mL of
854 culture was frozen at -20°C).
855
856 Whole-population, whole-genome sequencing, and analysis
857 DNA was extracted from frozen cell pellets using the DNeasy blood and tissue kit for the
858 QIAcube (Qiagen, Hilden, Germany) with a 10-minute elution into nuclease-free water. Libraries
859 were prepared in-house as previously described (20, 21) or using the plexWell™ kit following
860 manufacturer's directions (SeqWell PW096). Libraries were sequenced using an Illumina
861 NextSeq550 sequencer with a 300 cycle mid-output kit (Illumina 20024905). Reads were
862 demultiplexed, trimmed, and quality checked as described in the supplemental methods for the
863 RNAseq reads. Raw reads are uploaded to NCBI BioProject ID PRJNA1214285. Breseq (v0.35.0)
864 was used for read mapping and variant calling (22) with subsequent filtering following
865 previously published rationale (18) with special attention to new junction calls. Filtering,
866 consolidating for allele frequencies, and plotting were done in RStudio (R v4.2.1) with the
867 packages ggplot2 (v3.4.2; https://CRAN.R-project.org/package=ggplot2) and
868 tidyr (v1.3.0; https://CRAN.R-project.org/package=tidyr).
869
870 Growth curves as measure of fitness
871 We use bacterial growth curves to measure absolute fitness of ancestral clonal samples
872 as well as to measure aggregate absolute fitness of evolved populations (23). Growth curves
873 were seeded to mimic the transfers of the evolution experiment. A large sample of the frozen
874 population (or ancestor) stock was inoculated, in biological triplicate, into M9plus media and
875 grown for 24h. Overnight cultures were then diluted 1:100 into fresh media and OD600
876 measured every 10 minutes for 24h. Fitness was measured, in technical triplicate, in plain
877 M9plus as well as in M9plus containing 0.06 µg/mL TGC. We use area under the curve (AUC) to
878 measure fitness of populations normalized by the AUC of their respective ancestor ($AUC_{evolved}$
879 $_{population}$/$AUC_{ancestor\ average}$). Analyses were done in RStudio (R v4.2.1) utilizing previously
880 published pipelines (24) (https://github.com/mjfritz/Growth_Curves_in_R).
881
882 Quantitative reverse transcriptive PCR
883 To measure evolved efflux pump expression, we extracted RNA as described above for
884 ancestors and day-12 TGC evolved populations grown in the presence (0.06 µg/mL TGC,

885 ancestral cultures only) or absence of TGC (for ancestral and evolved populations). 50ng of
886 purified RNA was added per reaction for Q-RT-PCR according to manufacturer's instructions for
887 the Power SYBR Green RNA-to-Ct 1-Step Kit (Applied Biosystems). Reactions were performed in
888 biological and technical triplicate and run on a QuantStudio3 thermocycler using the default
889 threshold detection. Reactions lacking reverse transcriptase mix were included as controls for
890 DNA contamination. Data were analyzed for ΔCt and ΔΔCt, normalized by *rpoB* and ancestor,
891 respectively, within strain background. Expression values are presented as $2^{-\text{normalized expression}}$
892 such that higher values indicate increased expression. We used the main efflux pump gene
893 (*adeB, G, and J)* as a representative for pump expression (25, 26). Primers were designed with
894 Geneious to amplify approximately 150 base pair regions and are listed in Table S4.
895
896 Ethidium bromide efflux activity assay
897 Efflux activity was measured with the ethidium bromide uptake assay loosely based on
898 previously published methods (27). Ancestral cultures were grown overnight in M9plus, either
899 with or without addition of 0.06 µg/mL TGC, but not until saturation, and 500 µL was pelleted,
900 washed twice, and resuspended with PBS. Efflux activity of day-12 TGC-evolved populations
901 was measured only in untreated M9plus. A black flat-bottom 96-well plate (Corning ref. 3925)
902 was seeded with 90 µL of resuspended cells and 10 µL of 10 µg/mL ethidium bromide
903 (Invitrogen by Thermo Fisher Scientific ref. 15585-011). Fluorescence intensity was measured at
904 three minutes post addition of ethidium bromide with an excitation of 530 nm and emission of
905 600 nm. High efflux activity would result in a low fluorescence intensity as less ethidium
906 bromide is left within the cells binding to DNA. We present efflux activity as 1/RFU such that
907 higher values indicate more efflux. Efflux activity of the day-12 TGC-evolved populations when
908 grown in the untreated state relative to respective ancestor was calculated as
909 $1/(RFU_{query}/RFU_{untreated\ ancestor})$. Efflux activity was measured in biological triplicate with at least
910 three technical replicates each.
911
912
913

Main Text Citations

1. B. Aslam, *et al.*, Antibiotic resistance: a rundown of a global crisis. *Infect. Drug Resist.* **11**, 1645–1658 (2018).

2. M. Lässig, V. Mustonen, A. M. Walczak, Predicting evolution. *Nat. Ecol. Evol.* **1**, 77 (2017).

3. T. Gabaldón, Nothing makes sense in drug resistance except in the light of evolution. *Curr. Opin. Microbiol.* **75**, 102350 (2023).

4. A. C. Palmer, R. Kishony, Understanding, predicting and manipulating the genotypic evolution of antibiotic resistance. *Nat. Rev. Genet.* **14**, 243–248 (2013).

5. M. Travisano, J. A. Mongold, A. F. Bennett, R. E. Lenski, Experimental tests of the roles of adaptation, chance, and history in evolution. *Science* **267**, 87–90 (1995).

6. J. Plucain, *et al.*, Contrasting effects of historical contingency on phenotypic and genomic trajectories during a two-step evolution experiment with bacteria. *BMC Evol. Biol.* **16**, 86 (2016).

7. R. C. MacLean, A. San Millan, The evolution of antibiotic resistance. *Science* **365**, 1082–1083 (2019).

8. Z. D. Blount, R. E. Lenski, J. B. Losos, Contingency and determinism in evolution: Replaying life's tape. *Science* **362** (2018).

9. A. Santos-Lopez, *et al.*, The roles of history, chance, and natural selection in the evolution of antibiotic resistance. *eLife* **10** (2021).

10. L. Garoff, *et al.*, Population Bottlenecks Strongly Influence the Evolutionary Trajectory to Fluoroquinolone Resistance in Escherichia coli. *Mol. Biol. Evol.* **37**, 1637–1646 (2020).

11. A. Wong, Epistasis and the evolution of antimicrobial resistance. *Front. Microbiol.* **8**, 246 (2017).

12. R. C. MacLean, Predicting epistasis: an experimental test of metabolic control theory with bacterial transcription and translation. *J. Evol. Biol.* **23**, 488–493 (2010).

13. Z. D. Blount, A case study in evolutionary contingency. *Stud. Hist. Philos. Biol. Biomed. Sci.* **58**, 82–92 (2016).

14. G. J. Vermeij, Historical contingency and the purported uniqueness of evolutionary innovations. *Proc Natl Acad Sci USA* **103**, 1804–1809 (2006).

944 15. Y. Wang, *et al.*, Benefit of transferred mutations is better predicted by the fitness of
945 recipients than by their ecological or genetic relatedness. *Proc Natl Acad Sci USA* **113**,
946 5047–5052 (2016).

947 16. S. Dionisi, J. S. Huisman, Digest: The importance of genetic background in bacterial
948 evolution. *Evolution* **78**, 593–594 (2024).

949 17. N. Filipow, S. Mallon, S. Shewaramani, R. Kassen, A. Wong, The impact of genetic
950 background during laboratory evolution of Pseudomonas aeruginosa in a cystic fibrosis-
951 like environment. *Evolution* **78**, 566–578 (2024).

952 18. S. Cisneros-Mayoral, L. Graña-Miraglia, D. Pérez-Morales, R. Peña-Miller, A. Fuentes-
953 Hernández, Evolutionary history and strength of selection determine the rate of
954 antibiotic resistance adaptation. *Mol. Biol. Evol.* **39** (2022).

955 19. K. J. Card, T. LaBar, J. B. Gomez, R. E. Lenski, Historical contingency in the evolution of
956 antibiotic resistance after decades of relaxed selection. *PLoS Biol.* **17**, e3000397 (2019).

957 20. T. N. Batarseh, S. N. Batarseh, A. Rodríguez-Verdugo, B. S. Gaut, Phenotypic and
958 Genotypic Adaptation of Escherichia coli to Thermal Stress is Contingent on Genetic
959 Background. *Mol. Biol. Evol.* **40** (2023).

960 21. K. M. Flynn, T. F. Cooper, F. B.-G. Moore, V. S. Cooper, The environment affects epistatic
961 interactions to alter the topology of an empirical fitness landscape. *PLoS Genet.* **9**,
962 e1003426 (2013).

963 22. F. Baquero, *et al.*, Evolutionary pathways and trajectories in antibiotic resistance. *Clin.*
964 *Microbiol. Rev.* **34**, e0005019 (2021).

965 23. C.-R. Lee, *et al.*, Biology of Acinetobacter baumannii: Pathogenesis, Antibiotic Resistance
966 Mechanisms, and Prospective Treatment Options. *Front. Cell. Infect. Microbiol.* **7**, 55
967 (2017).

968 24. M. Touchon, *et al.*, The genomic diversification of the whole Acinetobacter genus:
969 origins, mechanisms, and consequences. *Genome Biol. Evol.* **6**, 2866–2882 (2014).

970 25. A. Iovleva, *et al.*, Carbapenem-Resistant Acinetobacter baumannii in U.S. Hospitals:
971 Diversification of Circulating Lineages and Antimicrobial Resistance. *MBio* **13**, e0275921
972 (2022).

973 26. M. J. Dorman, N. R. Thomson, “Community evolution” - laboratory strains and pedigrees
974 in the age of genomics. *Microbiology (Reading, Engl)* **166**, 233–238 (2020).

975 27. M. Del Mar Cendra, E. Torrents, Differential adaptability between reference strains and
976 clinical isolates of Pseudomonas aeruginosa into the lung epithelium intracellular
977 lifestyle. *Virulence* **11**, 862–876 (2020).

978 28. G. Makke, *et al.*, Whole-Genome-Sequence-Based Characterization of Extensively Drug-
979 Resistant Acinetobacter baumannii Hospital Outbreak. *mSphere* **5** (2020).

980 29. C. H. Camargo, *et al.*, Clonal spread of ArmA- and OXA-23-coproducing Acinetobacter
981 baumannii International Clone 2 in Brazil during the first wave of the COVID-19
982 pandemic. *J. Med. Microbiol.* **71** (2022).

983 30. M. Marazzato, *et al.*, Genetic Diversity of Antimicrobial Resistance and Key Virulence
984 Features in Two Extensively Drug-Resistant Acinetobacter baumannii Isolates. *Int. J.*
985 *Environ. Res. Public Health* **19** (2022).

986 31. M. R. Galac, *et al.*, A Diverse Panel of Clinical Acinetobacter baumannii for Research and
987 Development. *Antimicrob. Agents Chemother.* **64** (2020).

988 32. T. van Opijnen, S. Dedrick, J. Bento, Strain Dependent Genetic Networks for Antibiotic-
989 Sensitivity in a Bacterial Pathogen with a Large Pan-Genome. *PLoS Pathog.* **12**, e1005869
990 (2016).

991 33. L. Rizzetto, *et al.*, Strain dependent variation of immune responses to A. fumigatus:
992 definition of pathogenic species. *PLoS ONE* **8**, e56651 (2013).

993 34. J. Davies, D. Davies, Origins and evolution of antibiotic resistance. *Microbiol. Mol. Biol.*
994 *Rev.* **74**, 417–433 (2010).

995 35. A. Kaul, C. Souque, M. Holland, M. Baym, Genomic resistance in historical clinical isolates
996 increased in frequency and mobility after the age of antibiotics. *BioRxiv* (2025)
997 https:/doi.org/10.1101/2025.01.16.633422.

998 36. A. P. Hendry, Prediction in ecology and evolution. *Bioscience* (2023)
999 https:/doi.org/10.1093/biosci/biad083.

1000 37. K. E. Erickson, P. B. Otoupal, A. Chatterjee, Transcriptome-Level Signatures in Gene
1001 Expression and Gene Expression Variability during Bacterial Adaptive Evolution. *mSphere*
1002 **2** (2017).

1003 38. C. D. M. Wijers, *et al.*, Identification of Two Variants of Acinetobacter baumannii Strain
1004 ATCC 17978 with Distinct Genotypes and Phenotypes. *Infect. Immun.* **89**, e0045421
1005 (2021).

1006 39. P. Baumann, M. Doudoroff, R. Y. Stanier, A study of the Moraxella group. II. Oxidative-
1007 negative species (genus Acinetobacter). *J. Bacteriol.* **95**, 1520–1541 (1968).

1008 40. A. C. Jacobs, *et al.*, AB5075, a Highly Virulent Isolate of Acinetobacter baumannii, as a
1009 Model Strain for the Evaluation of Pathogenesis and Antimicrobial Treatments. *MBio* **5**,
1010 e01076-14 (2014).

1011 41. L. A. Gallagher, *et al.*, Resources for Genetic and Genomic Analysis of Emerging Pathogen
1012 Acinetobacter baumannii. *J. Bacteriol.* **197**, 2027–2035 (2015).

1013 42. N. D. Greer, Tigecycline (Tygacil): the first in the glycylcycline class of antibiotics. *Proc*
1014 *(Bayl Univ Med Cent)* **19**, 155–161 (2006).

1015 43. X. Hua, *et al.*, Novel tigecycline resistance mechanisms in Acinetobacter baumannii
1016 mediated by mutations in adeS, rpoB and rrf. *Emerg. Microbes Infect.* **10**, 1404–1417
1017 (2021).

1018 44. K. Lucaßen, *et al.*, Prevalence of RND efflux pump regulator variants associated with
1019 tigecycline resistance in carbapenem-resistant Acinetobacter baumannii from a
1020 worldwide survey. *J. Antimicrob. Chemother.* **76**, 1724–1730 (2021).

1021 45. X. Hua, Q. Chen, X. Li, Y. Yu, Global transcriptional response of Acinetobacter baumannii
1022 to a subinhibitory concentration of tigecycline. *Int. J. Antimicrob. Agents* **44**, 337–344
1023 (2014).

1024 46. L. Gao, X. Ma, Transcriptome Analysis of Acinetobacter baumannii in Rapid Response to
1025 Subinhibitory Concentration of Minocycline. *Int. J. Environ. Res. Public Health* **19** (2022).

1026 47. A. Santos-Lopez, C. W. Marshall, M. R. Scribner, D. J. Snyder, V. S. Cooper, Evolutionary
1027 pathways to antibiotic resistance are dependent upon environmental structure and
1028 bacterial lifestyle. *eLife* **8** (2019).

1029 48. T. Vogwill, M. Kojadinovic, R. C. MacLean, Epistasis between antibiotic resistance
1030 mutations and genetic background shape the fitness effect of resistance across species
1031 of Pseudomonas. *Proc. Biol. Sci.* **283** (2016).

1032 49. T. Vogwill, R. C. MacLean, The genetic basis of the fitness costs of antimicrobial
1033 resistance: a meta-analysis approach. *Evol. Appl.* **8**, 284–295 (2015).

1034 50. K. J. Card, J. A. Jordan, R. E. Lenski, Idiosyncratic variation in the fitness costs of
1035 tetracycline-resistance mutations in Escherichia coli. *Evolution* **75**, 1230–1238 (2021).

1036 51. M. R. Scribner, A. Santos-Lopez, C. W. Marshall, C. Deitrick, V. S. Cooper, Parallel
1037 Evolution of Tobramycin Resistance across Species and Environments. *MBio* **11** (2020).

1038 52. K. B. Harris, K. M. Flynn, V. S. Cooper, Polygenic adaptation and clonal interference
1039 enable sustained diversity in experimental Pseudomonas aeruginosa populations. *Mol.*
1040 *Biol. Evol.* (2021) https:/doi.org/10.1093/molbev/msab248.

1041 53. Q. Chen, *et al.*, Decreased susceptibility to tigecycline in Acinetobacter baumannii
1042 mediated by a mutation in trm encoding SAM-dependent methyltransferase. *J.*
1043 *Antimicrob. Chemother.* **69**, 72–76 (2014).

1044 54. S. Sharma, V. Kaushik, M. Kulshrestha, V. Tiwari, Different Efflux Pump Systems in
1045 Acinetobacter baumannii and Their Role in Multidrug Resistance. *Adv. Exp. Med. Biol.*
1046 **1370**, 155–168 (2023).

1047 55. I. V. Leus, *et al.*, Substrate Specificities and Efflux Efficiencies of RND Efflux Pumps of
1048 Acinetobacter baumannii. *J. Bacteriol.* **200** (2018).

1049 56. S. Raza, *et al.*, Molecular Characterization of Resistance-Nodulation-cell Division Efflux
1050 Pump Genes in Multidrug-Resistant Acinetobacter baumannii. *J. Glob. Infect. Dis.* **13**,
1051 177–179 (2021).

1052 57. S. Coyne, P. Courvalin, B. Périchon, Efflux-mediated antibiotic resistance in
1053 Acinetobacter spp. *Antimicrob. Agents Chemother.* **55**, 947–953 (2011).

1054 58. W. Huo, *et al.*, Immunosuppression broadens evolutionary pathways to treatment
1055 failure during *Acinetobacter baumannii* pneumonia. *BioRxiv* (2021)
1056 https:/doi.org/10.1101/2021.04.07.438861.

1057 59. N. Harmand, R. Gallet, G. Martin, T. Lenormand, Evolution of bacteria specialization
1058 along an antibiotic dose gradient. *Evol. Lett.* **2**, 221–232 (2018).

1059 60. L. Praski Alzrigat, D. L. Huseby, G. Brandis, D. Hughes, Resistance/fitness trade-off is a
1060 barrier to the evolution of MarR inactivation mutants in Escherichia coli. *J. Antimicrob.*
1061 *Chemother.* **76**, 77–83 (2021).

1062 61. B. R. Levin, V. Perrot, N. Walker, Compensatory mutations, antibiotic resistance and the
1063 population genetics of adaptive evolution in bacteria. *Genetics* **154**, 985–997 (2000).

1064 62. E. M. Darby, V. N. Bavro, S. Dunn, A. McNally, J. M. A. Blair, RND pumps across the genus
1065 Acinetobacter: AdeIJK is the universal efflux pump. *Microb. Genom.* **9** (2023).

1066 63. S. Gaiarsa, *et al.*, Can Insertion Sequences Proliferation Influence Genomic Plasticity?
1067 Comparative Analysis of Acinetobacter baumannii Sequence Type 78, a Persistent Clone
1068 in Italian Hospitals. *Front. Microbiol.* **10**, 2080 (2019).

1069 64. M. S. Wright, S. Mountain, K. Beeri, M. D. Adams, Assessment of Insertion Sequence
1070 Mobilization as an Adaptive Response to Oxidative Stress in Acinetobacter baumannii
1071 Using IS-seq. *J. Bacteriol.* **199** (2017).

1072 65. B. H. Good, I. M. Rouzine, D. J. Balick, O. Hallatschek, M. M. Desai, Distribution of fixed
1073 beneficial mutations and the rate of adaptation in asexual populations. *Proc Natl Acad*
1074 *Sci USA* **109**, 4950–4955 (2012).

1075 66. M. M. Desai, D. S. Fisher, Beneficial mutation selection balance and the effect of linkage
1076 on positive selection. *Genetics* **176**, 1759–1798 (2007).

1077 67. O. Schwengers, *et al.*, Bakta: rapid and standardized annotation of bacterial genomes via
1078 alignment-free sequence identification. *Microb. Genom.* **7** (2021).

1079 68. G. Tonkin-Hill, *et al.*, Producing polished prokaryotic pangenomes with the Panaroo
1080 pipeline. *Genome Biol.* **21**, 180 (2020).

1081 69. L. Pritchard, R. H. Glover, S. Humphris, J. G. Elphinstone, I. K. Toth, Genomics and
1082 taxonomy in diagnostics for food security: soft-rotting enterobacterial plant pathogens.
1083 *Anal. Methods* **8**, 12–24 (2016).

1084 70. K. A. Jolley, M. C. J. Maiden, BIGSdb: Scalable analysis of bacterial genome variation at
1085 the population level. *BMC Bioinformatics* **11**, 595 (2010).

1086 71. M. Feldgarden, *et al.*, AMRFinderPlus and the Reference Gene Catalog facilitate
1087 examination of the genomic links among antimicrobial resistance, stress response, and
1088 virulence. *Sci. Rep.* **11**, 12728 (2021).

1089 72. C. CLSI, *M100: Performance Standards for Antimicrobial Susceptibility Testing*, 32nd Ed.
1090 (Clinical and Laboratory Standards Institute, 2022).

1091 73. N. L. Bray, H. Pimentel, P. Melsted, L. Pachter, Near-optimal probabilistic RNA-seq
1092 quantification. *Nat. Biotechnol.* **34**, 525–527 (2016).

1093 74. M. I. Love, W. Huber, S. Anders, Moderated estimation of fold change and dispersion for
1094 RNA-seq data with DESeq2. *Genome Biol.* **15**, 550 (2014).

1095 75. A. Santos-Lopez, *et al.*, Evolved resistance to a novel cationic peptide antibiotic requires
1096 high mutation supply. *Evol. Med. Public Health* **10**, 266–276 (2022).

1097 76. C. B. Turner, C. W. Marshall, V. S. Cooper, Parallel genetic adaptation across
1098 environments differing in mode of growth or resource availability. *Evol. Lett.* **2**, 355–367
1099 (2018).

1100 77. D. E. Deatherage, J. E. Barrick, Identification of mutations in laboratory-evolved
1101 microbes from next-generation sequencing data using breseq. *Methods Mol. Biol.* **1151**,
1102 165–188 (2014).

1103 78. A. Alonso-Del Valle, *et al.*, Variability of plasmid fitness effects contributes to plasmid
1104 persistence in bacterial communities. *Nat. Commun.* **12**, 2653 (2021).

1105 79. M. J. Muraski, *et al.*, Adaptation to Overflow Metabolism by Mutations That Impair tRNA
1106 Modification in Experimentally Evolved Bacteria. *MBio* **14**, e0028723 (2023).

1107 80. F. Lin, *et al.*, Molecular Characterization of Reduced Susceptibility to Biocides in Clinical
1108 Isolates of Acinetobacter baumannii. *Front. Microbiol.* **8**, 1836 (2017).
1109
1110

1111 Supplemental Methods Citations

1112 1. C. D. M. Wijers, *et al.*, Identification of Two Variants of Acinetobacter baumannii
1113 Strain ATCC 17978 with Distinct Genotypes and Phenotypes. *Infect. Immun.* **89**,
1114 e0045421 (2021).

1115 2. P. Baumann, M. Doudoroff, R. Y. Stanier, A study of the Moraxella group. II.
1116 Oxidative-negative species (genus Acinetobacter). *J. Bacteriol.* **95**, 1520–1541
1117 (1968).

1118 3. A. C. Jacobs, *et al.*, AB5075, a Highly Virulent Isolate of Acinetobacter baumannii,
1119 as a Model Strain for the Evaluation of Pathogenesis and Antimicrobial Treatments.
1120 *MBio* **5**, e01076-14 (2014).

1121 4. L. A. Gallagher, *et al.*, Resources for Genetic and Genomic Analysis of Emerging
1122 Pathogen Acinetobacter baumannii. *J. Bacteriol.* **197**, 2027–2035 (2015).

1123 5. A. Santos-Lopez, C. W. Marshall, M. R. Scribner, D. J. Snyder, V. S. Cooper,
1124 Evolutionary pathways to antibiotic resistance are dependent upon environmental
1125 structure and bacterial lifestyle. *eLife* **8** (2019).

1126 6. O. Schwengers, *et al.*, Bakta: rapid and standardized annotation of bacterial
1127 genomes via alignment-free sequence identification. *Microb. Genom.* **7** (2021).

1128 7. G. Tonkin-Hill, *et al.*, Producing polished prokaryotic pangenomes with the Panaroo
1129 pipeline. *Genome Biol.* **21**, 180 (2020).

1130 8. L. Pritchard, R. H. Glover, S. Humphris, J. G. Elphinstone, I. K. Toth, Genomics and
1131 taxonomy in diagnostics for food security: soft-rotting enterobacterial plant
1132 pathogens. *Anal. Methods* **8**, 12–24 (2016).

1133 9. K. A. Jolley, M. C. J. Maiden, BIGSdb: Scalable analysis of bacterial genome
1134 variation at the population level. *BMC Bioinformatics* **11**, 595 (2010).

1135 10. M. Feldgarden, *et al.*, AMRFinderPlus and the Reference Gene Catalog facilitate
1136 examination of the genomic links among antimicrobial resistance, stress response,
1137 and virulence. *Sci. Rep.* **11**, 12728 (2021).

1138 11. R. L. Tatusov, M. Y. Galperin, D. A. Natale, E. V. Koonin, The COG database: a tool
1139 for genome-scale analysis of protein functions and evolution. *Nucleic Acids Res.*
1140 **28**, 33–36 (2000).

1141 12. C. CLSI, *M100: Performance Standards for Antimicrobial Susceptibility Testing*,
1142 32nd Ed. (Clinical and Laboratory Standards Institute, 2022).

1143 13. A. C. Stephens, L. R. Thurlow, A. R. Richardson, Mechanisms Behind the Indirect
1144 Impact of Metabolic Regulators on Virulence Factor Production in Staphylococcus
1145 aureus. *Microbiol. Spectr.* **10**, e0206322 (2022).

1146 14. N. L. Bray, H. Pimentel, P. Melsted, L. Pachter, Near-optimal probabilistic RNA-seq
1147 quantification. *Nat. Biotechnol.* **34**, 525–527 (2016).

1148 15. M. I. Love, W. Huber, S. Anders, Moderated estimation of fold change and
1149 dispersion for RNA-seq data with DESeq2. *Genome Biol.* **15**, 550 (2014).

1150 16. T. Bliek, J. Chouaref, F. van der Kloet, J. Szkodon, M. Galland, *Introductionto RNA-*
1151 *seq lesson* (2020) (July 1, 2024).

1152 17. A. Zhu, J. G. Ibrahim, M. I. Love, Heavy-tailed prior distributions for sequence count
1153 data: removing the noise and preserving large differences. *Bioinformatics* **35**, 2084–
1154 2092 (2019).

1155 18. M. R. Scribner, A. Santos-Lopez, C. W. Marshall, C. Deitrick, V. S. Cooper, Parallel
1156 Evolution of Tobramycin Resistance across Species and Environments. *MBio* **11**
1157 (2020).

1158 19. A. Santos-Lopez, *et al.*, Evolved resistance to a novel cationic peptide antibiotic
1159 requires high mutation supply. *Evol. Med. Public Health* **10**, 266–276 (2022).

1160 20. M. Baym, *et al.*, Inexpensive multiplexed library preparation for megabase-sized
1161 genomes. *PLoS ONE* **10**, e0128036 (2015).

1162 21. C. B. Turner, C. W. Marshall, V. S. Cooper, Parallel genetic adaptation across
1163 environments differing in mode of growth or resource availability. *Evol. Lett.* **2**, 355–
1164 367 (2018).

1165 22. D. E. Deatherage, J. E. Barrick, Identification of mutations in laboratory-evolved
1166 microbes from next-generation sequencing data using breseq. *Methods Mol. Biol.*
1167 **1151**, 165–188 (2014).

1168 23. A. Alonso-Del Valle, *et al.*, Variability of plasmid fitness effects contributes to
1169 plasmid persistence in bacterial communities. *Nat. Commun.* **12**, 2653 (2021).

1170 24. M. J. Muraski, *et al.*, Adaptation to Overflow Metabolism by Mutations That Impair
1171 tRNA Modification in Experimentally Evolved Bacteria. *MBio* **14**, e0028723 (2023).

1172 25. S. Coyne, P. Courvalin, B. Périchon, Efflux-mediated antibiotic resistance in
1173 Acinetobacter spp. *Antimicrob. Agents Chemother.* **55**, 947–953 (2011).

1174 26. F. Lin, *et al.*, Molecular Characterization of Reduced Susceptibility to Biocides in
1175 Clinical Isolates of Acinetobacter baumannii. *Front. Microbiol.* **8**, 1836 (2017).

1176 27. Z. R. Lonergan, *et al.*, An Acinetobacter baumannii, Zinc-Regulated Peptidase
1177 Maintains Cell Wall Integrity during Immune-Mediated Nutrient Sequestration. *Cell*
1178 *Rep.* **26**, 2009-2018.e6 (2019).

1179